Potential of Vesicles to Optimize Topically Applied Formulations with Enhanced Skin Penetration of Drugs

2017

Pajaree Sakdiset

Contents

Abbreviations

CPEs	Chemical penetration enhancers
SC	Stratum corneum
SCLL	Stratum corneum lipid liposome
HTS	High-throughput screening
T_m	Transition temperature
DSC	Differential scanning calorimetry
FL	Sodium fluorescein
DPH	1,6-Diphenyl-1,3,5-hexatriene
TMA-DPH	*N*,*N*,*N*-trimethyl-4-(6-phenyl-1,3,5-hexatrien-1-yl)phenyl-ammonium *p*-toluenesulfonate
ANS	8-Anilino-1-naphthalenesulfonic acid ammonium salt
CER[NP]	*N*-(octadecanoyl)-phytosphingosine
CER[AP]	*N*-(α-hydroxyoctadecanoyl)-phytosphingosine
PEG	Polyethylene glycol
PBS	Phosphate-buffered saline pH 7.4
HPLC	High-performance liquid chromatography
ER	Skin penetration-enhancement ratio
Q	Cumulative amount of drug permeated per unit area of skin
FL-SCLLs	Stratum corneum lipid liposome containing sodium fluorescein
P_f	Fluorescence polarization
DPH-SCLL	Stratum corneum lipid liposome containing DPH.
$EC_{10,\ leakage}$	Effective concentration for promoting 10% FL leakage
$EC_{10,\ fluidity}$	Effective concentration for promoting 10% increase in SCLL fluidity
Log $K_{o/w}$	Logarithmic of octanol/ water partition coefficient
HLB	Hydrophile-lipophile balance
R^2	Coefficient of determination
DLPC	1,2-Dilauroyl-*sn*-glycero-3-phosphocholine
DMPC	1,2-Dimyristoyl-*sn*-glycero-3-phosphocholine
DPPC	1,2-Dipalmitoyl-*sn*-glycero-3-phosphocholine
DSPC	1,2-Distearoyl-*sn*-glycero-3-phosphocholine
DOPC	1,2-Dioleoyl-*sn*-glycero-3-phosphocholine

DLPG	1,2-Dilauroyl-*sn*-glycero-3-phosphoglycerol, sodium salt
DMPG	1,2-Dimyristoyl-*sn*-glycero-3-phosphoglycerol, sodium salt
DPPG	1,2-Dipalmitoyl-*sn*-glycero-3-phosphoglycerol, sodium salt
DSPG	1,2-Distearoyl-*sn*-glycero-3-phosphoglycerol, sodium salt
DOPG	1,2-Dioleoyl-*sn*-glycero-3-phosphoglycerol, sodium salt
EE	Entrapment efficiency
E_{drug}	Entrapped drug
U_{drug}	Unentrapped drug
T_{drug}	Total drug

Abstract

In the field of transdermal and topical drug delivery, vesicles have gained high interest in the past few decades. Vesicles could be used as a model skin membrane, *e.g*. stratum corneum lipid liposomes (SCLLs), as well as drug delivery carriers, *e.g.* liposomes and niosomes. In the present study, these applications of vesicles were investigated.

In the first chapter, SCLLs were prepared to serve as a model stratum corneum (SC) intercellular lipid to evaluate the effect of chemical penetration enhancers (CPEs) on the barrier function of SC lipid. A fluorescent probe; sodium fluorescein (FL) was entrapped in SCLLs for investigation of the FL leakage from SCLLs. Also, 1,6-diphenyl-1,3,5-hexatriene (DPH), *N*,*N*,*N*-trimethyl-4-(6-phenyl-1,3,5-hexatrien-1-yl)phenyl-ammonium *p*-toluenesulfonate (TMA-DPH) or 8-anilino-1-naphthalenesulfonic acid ammonium salt (ANS) were separately entrapped in SCLLs for the measurement of SCLL membrane fluidity. The preliminary study was performed using ethanol as a model CPE. The relationship between the conventional animal assay (skin permeation/ skin impedance test) on hairless rat skin and the test based on SCLLs (FL leakage and SCLL membrane fluidity test) was evaluated. Fair correlations were obtained from the increase in enhancement ratio (*ER*) of caffeine permeation with FL leakage and SCLLs membrane fluidity measured using ANS probe with R^2 of 0.8882 and 0.8993, respectively. FL leakage and SCLLs membrane fluidity test measured using DPH probe were also performed with various types and concentrations of well-known CPEs. An effective concentration for promoting 10% FL leakage and increase in SCLLs membrane fluidity ($EC_{10,\ leakage}$ and $EC_{10,\ fluidity}$) were calculated by interpolation from their concentration profiles. The lipophilic CPEs tends to exhibit lower $EC_{10,\ leakage}$ and $EC_{10,\ fluidity}$ than hydrophilic CPEs. In addition, the relationship between FL leakage and SCLLs membrane fluidity were classified into five categories depending on the action on SCLLs. This method using SCLL as a model SC intercellular lipid could be utilized in investigating the effects of CPE on SC as an alternative high-throughput screening (HTS) technique in contrast to conventional animal testing.

In the second chapter, components of vesicles having high skin penetration-enhancing effect was selected to formulate new penetration-enhancing vesicles. The screening of phospholipids and non-ionic surfactants was performed using diffusion cell array system and abdominal skin of hairless rat. Caffeine was used as a hydrophilic model drug. The results showed a significant increase in *ER* from 1,2-distearoyl-*sn*-glycero-3-phosphocholine (DSPC),

1,2-dipalmitoyl-*sn*-glycero-3-phosphoglycerol, sodium salt (DPPG), Brij 30, Span 20, Tween 20, Tween 40 and Tween 60, compared to the control solution. The liposomes and niosomes prepared from varying compositions influenced particle size, transition temperature, entrapment efficiency and zeta potential. The vesicles exhibiting high *ER* were DPPG, 1,2-dilauroyl-*sn*-glycero-3-phosphocholine (DLPC), 1,2-dimyristoyl-*sn*-glycero-3-phosphocholine (DMPC) liposomes and Span 20, Tween 85 niosomes. In addition, two kinds of experiments were done to clarify the possible mechanism of liposomes as follows: the excised skin was pretreated for 1 h with caffeine-free phospholipid dispersions and liposomes, and caffeine solution was added to determine its skin permeation. Separately, caffeine permeation experiments were done using physical mixture of blank liposomes and caffeine solution (caffeine-spiked liposomes) and caffeine-entrapped liposomes (caffeine was entrapped only in liposomes). As a result, DPPG was found to be a promising phospholipid candidate to develop liposome formulations since it could significantly enhance the skin permeation of caffeine as in the pretreatment experiments. In addition, DPPG liposomes could carry both non-entrapped and entrapped caffeine through the skin. Thus, selecting the compositions of liposomes and niosomes is a crucial factor to consider in improving the skin penetration of drugs from the drug delivery carriers.

General Introduction

Skin is the largest human organ acting as a barrier against exogenous materials as well as controlling the homeostasis[1)]. Skin has been recognized as a site for topical application of drugs to expect local and/or systemic therapeutic effects with its non-invasiveness, control of release property, avoidance of gastrointestinal and first pass metabolism, and reduction of side effects associated with high oral dose and gastrointestinal distress[2,3)].

Due to the barrier properties of the skin, only low-dose and potent lipophilic drugs can be optimally delivered at therapeutic rates by passive diffusion[3)]. Thus, many approaches to overcome the barrier function of the skin were introduced in order to increase drug delivery into and through the skin such as prodrug approach, application of chemical penetration enhancers (CPEs), use of physical means such as iontophoresis, electroporation and microneedle, and drug delivery carrier approaches[4-6)]. Among them, the use of vesicles such as liposomes and niosomes is one of the approaches that have been extensively investigated to deliver drugs through skin. Vesicles can be defined as highly ordered assemblies of one or several concentric bilayers spontaneously formed when amphiphilic building blocks are surrounded with water[7)].

In the field of topical and transdermal drug delivery, several kinds of vesicles can be utilized as model membranes to mimic stratum corneum (SC) lipids as well as drug carriers to enhance delivery of drugs into and through the skin.

The usefulness of vesicles as model SC membrane has been already reported. Liposomal vesicles can be used as an alternative tool representing human and animal skin models, since liposomes show a multiple bilayered organization similar to the human SC intercellular lipid domains. Conventionally, the investigation of the skin penetration-enhancement effect of chemicals relies on the skin permeation study and/or skin impedance test using human or animal skin as test membranes[8,9)]. These methods are time consuming, expensive and associated with ethical issues. Therefore, liposome, as a SC lipid alternative, has been used to investigate the action of CPEs[10-12)].

The first chapter of the present study focused on the development of high-throughput screening (HTS) technique based on the SC lipid liposomes (SCLL), which were prepared using similar lipid compositions to SC lipid, for testing various types and concentrations of CPEs. This study was based on the ability of CPEs to promote the leakage and fluidity of the

SCLL due to the disruption on the lipid bilayers structure. The suitability of using liposomes as model SC membrane was evaluated by comparing with a conventional evaluation method for skin penetration-enhancing effects, *i.e.*, skin permeation experiment and skin impedance determination.

The second chapter of the present study was related to the usefulness of several vesicles as a drug carrier for topical and transdermal drug delivery, since vesicles provide various advantages; they can entrap both hydrophilic and lipophilic molecules, protect the encapsulated drug from chemical degradation, and control the drug release while having high skin permeability enhancement[13-15].

Several mechanisms on the skin penetration enhancement by vesicular carriers have been reported including intact vesicular skin penetration, penetration-enhancing effect, adsorption effect and penetration of liposomes through the transappendageal route[15]. Interestingly, the proposed mechanisms for skin penetration-enhancement effect of vesicles are related to the penetration of vesicle lipids into the SC and then destabilization, followed by fusion or mixing with the intercellular lipid matrix to loosen the packed intercellular lipid structure with subsequent increased skin partitioning of the drugs[16].

Since the composition of vesicles can also affect to their skin penetration-enhancing effects of drugs, the selection of the candidate amphiphilic compositions (phospholipids and non-ionic surfactants) is important for obtaining a high skin penetration-enhancing effect of the carriers. Hence, in the second chapter, a novel approach to formulate penetration-enhancement vesicles was developed. This approach is based on the selection of the vesicular carrier composition by *in vitro* skin permeation screening to assess the suitable compositions with high skin penetration-enhancement effect for a model hydrophilic drug, caffeine. Liposomes and niosomes were prepared and determined for the skin penetration-enhancing property. The obtained results were compared to those by aqueous dispersion of their phospholipids/non-ionic surfactants. In addition, the possible mechanisms for the high skin penetration-enhancing effect from vesicles were investigated.

Chapter 1

Potential of stratum corneum lipid liposome as a tool for screening of chemical penetration enhancers

1.1. Introduction

Skin is of considerable interest as an administration route for drugs with both local and systemic effects. However, the main obstacle for drugs to pass through the skin and exert their pharmacological activities is the intrinsic barrier function of the SC. The SC is the uppermost layer of the skin consisting of keratin-filled corneocytes and intercellular lipids[1,17]. Generally, drugs in vehicles applied topically onto the skin firstly distribute into the SC and then diffuse mainly through the intercellular lipid domain in the SC[18]. Because the intercellular lipids organize into multi-lamellar complexes filling the intercellular spaces to provide a strong barrier against the entry of the exogenous drugs[19], approaches to overcome the skin barrier function have been investigated extensively to improve the skin permeability of drugs.

Use of CPEs is a conventional and effective approach to overcome the high barrier function of the SC. They promote the skin permeation of drugs by reducing skin barrier resistance[20]. CPEs may disrupt intercellular lipids, or interact with intracellular proteins or with both regions in the SC[10]. Conventional CPEs have been screened using skin permeation experiments to determine the cumulative amount of skin permeation, flux and permeability coefficient of drugs in the presence and absence of CPEs[9]. However, these conventional approaches are time-consuming, complicated and resource expensive. These methods are not practical for HTS with various types and concentrations of CPEs as part of their discovery and development. In addition, increasing awareness of animal welfare issues nowadays has brought about a reduction in animal-based experiments, especially in the cosmetics industries. This situation gives rise to a need to develop an effective replacement approach that can provide HTS for effective CPEs as well as avoid the use of experimental animals.

SCLLs consist of a lipid mixture similar to SC multi-lamellar lipid bilayers that are composed of ceramides, cholesterol, cholesterol esters and fatty acids[19,21]. SCLLs have been used as an SC intercellular lipid mimicking model to investigate the effect of agents on the skin permeability and the mechanism of enhanced skin delivery[22,23]. One of the determination

procedures is based on the change in transition temperature (T_m) of SCLLs due to the chemicals determined by differential scanning calorimetry (DSC)[22]. However, this technique is also time-consuming, unable to simultaneously determine various samples and difficult to obtain quantitative data. SCLLs containing entrapped marker(s) (*e.g.* glucose, mannitol and calcein) have been applied to determine the release rate of the markers[12,22,24,25]. In addition, labeled fluorescent probes are also used to measure the fluidizing effect of CPEs on SCLLs[26]. However, these methods are still not appropriate for HTS of CPEs, because of the complicated analytical methods and rather long experimental time.

Thus, the aim of the present chapter was to establish a simple, quantitative, fast and practical approach for HTS of potential CPEs. Ethanol was used as a model CPE to firstly investigate the potential of SCLLs based on the HTS methodology, because it is well-known and is already used to increase the skin penetration of various drugs such as hydrocortisone, 5-fluorouracil and estradiol[27-29]. SCLLs entrapped of a hydrophilic fluorescent probe, sodium fluorescein (FL) and incubated with three fluorescent probes with different lipophilicities were used to observe SCLL leakage and fluidity, respectively, and compared with conventional *in vitro* skin permeation test as well as skin impedance test to determine the effectiveness of this HTS technology. Moreover, various types of well-known CPEs with different concentrations were determined for their effects on SCLL leakage and fluidity as well as categorized according to their concentration profiles and the mechanism of those CPEs action on SC lipids was proposed.

1.2. Materials and Methods

1.2.1. Materials

FL, lignoceric acid, palmitic acid, boric acid, potassium chloride, sodium hydroxide, chloroform, methanol, ethanol, *n*-propanol, Transcutol® (diethylene glycol monoethyl ether), dimethyl sulfoxide, oleic acid, ethyl oleate, sodium dodecyl sulfate, Brij® 58 and 1-methyl-2-pyrrolidone were purchased from Wako Pure Chemicals Industries, Ltd. (Osaka, Japan). Cholesterol, cholesteryl sulfate, octacosanoic acid, 1,6-diphenyl-1,3,5-hexatriene (DPH), *N*,*N*,*N*-trimethyl-4-(6-phenyl-1,3,5-hexatrien-1-yl)phenyl-ammonium *p*-toluenesulfonate (TMA-DPH), 8-anilino-1-naphthalenesulfonic acid ammonium salt (ANS) and Pluronic® F-127, were obtained from Sigma-Aldrich (St. Louis, MO, USA). CER[NP] (*N*-(octadecanoyl)-

phytosphingosine) and CER[AP] (*N*-(α-hydroxyoctadecanoyl)-phytosphingosine) were obtained from Evonik Industries AG (Essen, Germany). Sodium decanoate, 1,8-cineol, lauryl alcohol, cetylpyridinium chloride, polyoxyethylene sorbitan fatty acid esters (Tween 20, 40, 60, 80, 85) and sorbitan fatty acid esters (Span 20, 40, 60, 80) were obtained from Tokyo Chemical Industry Co., Ltd. (Tokyo, Japan). Propylene glycol, polyethylene glycol (PEG) 400 and benzyl alcohol were obtained from Kanto Chemical Co., Inc. (Tokyo, Japan). Sefsol 218 (propylene glycol monocaprylate) was a kind gift from Nikko Chemicals Co., Ltd. (Tokyo, Japan). Pluronic® P-84 was supplied by Adeka Corporation (Tokyo, Japan) and *l*-menthol was obtained from Fisher Scientific Japan (Tokyo, Japan). These reagents were used without further purification.

1.2.2. Experimental animals

Male WBN/ILA-Ht hairless rats, weighing between 200 and 260 g, were obtained from the Life Science Research Center, Josai University (Saitama, Japan) and Ishikawa Experimental Animal Laboratories (Saitama, Japan). Rats were bred in a room maintained at 25 ± 2°C, in which the on and off times for the lighting were 07:00 and 19:00, respectively. Animals had free access to water and food (MF, Oriental Yeast Co., Ltd., Tokyo, Japan).

All breeding procedures and experiments on the animals were performed in accordance with the guidelines of the Animal Experiment Committee of Josai University (Sakado, Saitama, Japan)

1.2.3. Measurement of skin impedance reduction rate

The mixture of three types of anesthesia (medetomidine, 0.375 mg/kg; butorphanol, 2.5 mg/kg; and midazolam, 2 mg/kg) was injected intraperitoneally into hairless rats. Hairs were removed from the back under anesthesia. The treated back skin was excised, and subcutaneous fat was removed carefully using scissors. The skin was mounted with the SC side up on a square-type diffusion cell with an effective area of 19.5 cm^2 and a receiver volume of 45 mL. Eight donor cells with an effective diffusion area of 0.795 cm^2 were glued with cyanoacrylate bond (Aron Alpha®, Konishi Co. Ltd., Osaka, Japan) onto the skin as shown in Fig. 1-1. Then, 1.0 and 45 mL physiological saline were added to the donor and receiver cells, respectively, to hydrate the skin. Skin impedance was then determined using an impedance meter (Asahi

Techno Lab., Ltd., Yokohama, Japan) 1 h after hydration. Thereafter, the physiological saline was removed from the donor cell and 1.0 mL of different concentrations of ethanol was applied for 1 h. At the end of the experiment, the donor solution was removed, the same volume of fresh saline was added and skin impedance was determined again. Reduction in the skin impedance (%) was calculated from the following equation.

$$\text{Reduction in the skin impedance (\%)} = \left(1 - \frac{\text{skin impedance after applied ethanol solution}}{\text{skin impedance after hydration}}\right) \text{x100} \qquad (1)$$

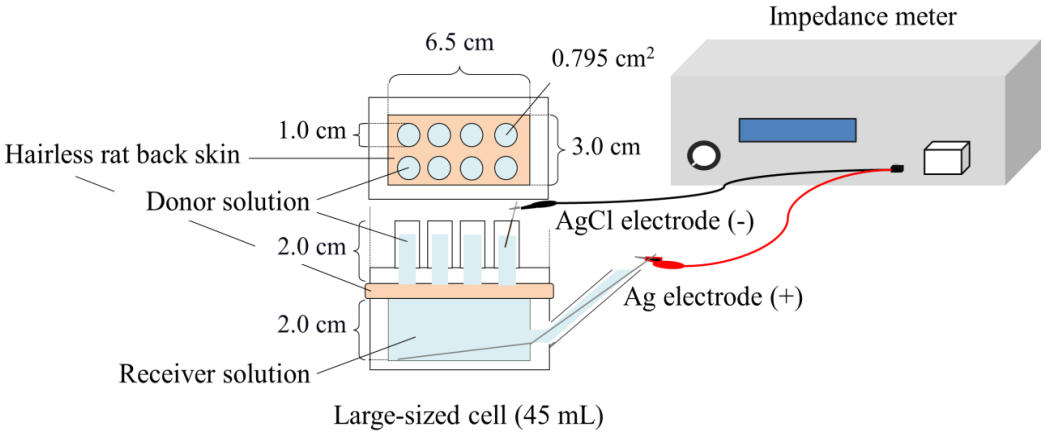

Fig. 1-1. Set-up of large-sized cell for skin impedance measurement.

1.2.4. In vitro skin permeation experiments

Excised abdominal skin from hairless rat was mounted in a vertical-type Franz diffusion cell (receiver cell volume 6.0 mL and effective permeation area 1.77 cm^2) with the SC side facing the donor cells and the dermal side facing the receiver cell. The receiver cell was filled with 6.0 mL phosphate-buffered saline pH 7.4 (PBS). PBS was also added to the donor cells for 1 h for skin hydration. Then, 0.5 mL of 2 mg/mL caffeine solution in 0, 10, 20, 30, 40, 50, 75 or 100% ethanol in PBS were applied to determine the skin permeation of caffeine at 32°C over 8 h while the receiver solution was agitated at 500 rpm using a magnetic stirrer. At predetermined times, 0.5 mL aliquots were collected and the same volume of PBS was added to keep the volume constant.

1.2.5. Determination of caffeine permeation

The concentration of caffeine was determined using a high-performance liquid chromatography (HPLC) system (Prominence, Shimadzu Corporation, Kyoto, Japan) equipped with a UV detector (SPD-M20A, Shimadzu Corporation). Briefly, the receiving solutions were mixed with the same volume of methanol. After centrifugation at 21,500 × *g* at 4°C for 5 min, the resulting supernatant (20 µL) was injected directly into the HPLC system. Chromatographic separation was performed at 40°C using an Inertsil ODS-3, 5 µm in diameter, 4.6 mm I.D. x 150 mm (GL Sciences Inc., Tokyo, Japan). The mobile phase was 0.1% phosphoric acid:methanol 7:3 v/v and the flow rate was 1.0 mL/min. UV absorbance detection was performed at 280 nm. The increase in the skin penetration-enhancement ratio (*ER*) after 8 h-permeation experiment was calculated using the following equation.

$$\text{Increase in } ER = \left(\frac{Q_{sample} - Q_{control}}{Q_{control}}\right) \quad (2)$$

where Q_{sample} and $Q_{control}$ are the cumulative amount of caffeine permeated per unit area of skin over 8 h from different concentrations of ethanol and PBS, respectively.

1.2.6. Preparation of SCLLs

SCLLs were prepared using the thin film hydration method reported by Hatfield and Fung (1999)[30] with a slight modification. Total lipids (5.5 mg/mL), which include 33% CER[NP], 22% CER[AP], 25% cholesterol, 5% cholesteryl sulfate, 7.5% lignoceric acid, 3.75% palmitic acid, and 3.75% octacosanoic acid were first dissolved in chloroform:methanol (2:1) in a round-bottomed flask. The solvent was then evaporated at 60°C under reduced pressure using a rotary evaporator until a thin film was obtained on the wall of the flask. The flask was then purged with N_2 gas and allowed to stand overnight to remove any traces of organic solvents. Next, the lipid film was annealed in a water bath at 90°C for 30 min. FL in 0.1 M borate buffer pH 9.0 (2.5 mg/mL) for FL-SCLLs or plain buffer for blank-SCLLs was used to hydrate the lipid film. The resulting SCLL suspension was then sonicated using a probe sonicator (VCX-750, Sonics & Materials Inc., Newtown, CT, USA) at an amplitude of 20% for 30 s. A freeze-thaw process was performed by immersing the flask in liquid N_2 and in a

water bath at 90°C, each for 3 min in 4 cycles. The obtained liposomes were further extruded using an extruder (Lipex™, Northern Lipids Inc., Burnaby, BC, Canada) with a membrane filter with pore sizes of 400, 200 and 100 nm (Nucleopore® track-etched membranes, GE Healthcare Japan, Tokyo, Japan), twice for each size of filter.

After preparation of FL-SCLLs, excess FL was removed by ultra-centrifugation (Hitachi CS100GXL, Hitachi Koki Co., Ltd., Tokyo, Japan) at 289,000 × *g*, 4°C twice for 15 min, twice for 10 min and 5 times for 5 min. At each centrifugation process, the supernatant was removed and the same volume of 0.1 M borate buffer was added and mixed.

1.2.7. Determination of FL leakage from SCLLs

FL-SCLLs were mixed 5 times by pipetting with different types and concentrations of CPEs solution in borate buffer, as shown in Table 1-1, at a ratio of FL-SCLLs: CPEs solution 1:9 v/v. However, 3% ethanol in borate buffer was used as solubilizing medium for oleic acid, ethyl oleate, Sefsol 218, lauryl alcohol, *l*-menthol and 1,8-cineol. Each sample was allowed to stand for 30 min at room temperature and immediately ultracentrifuged (Hitachi CS100GXL, Hitachi Koki Co., Ltd., Tokyo, Japan) at 289,000 × *g*, 4°C for 5 min. The supernatant was collected to determine the amount of FL that leaked from FL-SCLLs after mixing with CPEs solution (FL leakage), using a microplate reader (Spectra Max® M2^e, Molecular Devices, LLC., Sunnyvale, CA, USA) at excitation and emission wavelengths of 485 and 535 nm, respectively. This study was also performed using 75% ethanol and 0.1 M borate buffer to represent total and background FL leakage, respectively. A concentration of ethanol at 75% was found to totally disrupt the FL-SCLLs as no evidence of SCLL pellet precipitation was observed after the ultracentrifugation process. The calculation of FL leakage (%) is shown as follows:

$$\text{FL leakage (\%)} = \left(\frac{FL_{sample} - FL_{background}}{FL_{total} - FL_{background}}\right) \text{x } 100 \qquad (3)$$

Table 1-1. List of CPEs and their concentrations tested in this study

Group of enhancers	Enhancers	Concentration (%)
Anionic surfactant	Sodium dodecyl sulfate	0.01, 0.05, 0.1, 1.0, 2.5, 5.0
Cationic surfactant	Cetylpyridinium chloride	0.01, 0.05, 0.1, 1.0, 2.5, 5.0
Nonionic surfactant		
Polysorbates	Tween 20, 40, 60, 80, 85	0.01, 0.05, 0.1, 1.0, 2.5, 5.0
Sorbitans	Span 20, 40, 60, 80	0.01, 0.05, 0.1, 1.0, 2.5, 5.0
Brij	Brij 58	0.01, 0.05, 0.1, 1.0, 2.5, 5.0
Pluronic	Pluronic P-84, F-127	0.01, 0.05, 0.1, 1.0, 2.5, 5.0
Urea and its derivatives	Urea	5, 10, 20, 30, 40, 50
Glycols	PEG 400, Propylene glycol	5, 10, 20, 30, 40, 50, 75
	Transcutol	5, 10, 20, 30, 40, 50, 75
Short chain alcohols	Ethanol, *n*-Propanol	5, 10, 20, 30, 40, 50, 75
Aromatic ring alcohols	Benzyl alcohol	2.5, 5, 10
Fatty acids	Sodium decanoate	1, 5, 10, 20, 30
	Oleic acid, Ethyl oleate	0.01, 0.05, 0.1
Polyol fatty acid esters	Sefsol 218	0.01, 0.05, 0.1, 1, 2.5, 5
Fatty alcohols	Lauryl alcohol	0.01, 0.05, 0.1
Sulfoxides	Dimethyl sulfoxide	5, 10, 20, 30, 40, 50, 75
Pyrrolidones	1-Methyl-2-pyrrolidone	1, 5, 10, 20
Terpenes	*l*-Menthol, 1,8-Cineol	0.01, 0.05, 0.1, 1.0

1.2.8. Measurement of SCLLs membrane fluidity

The fluidity of the SCLL membranes was determined according to the method of Tan *et al*. (2016) with a slight modification[31]. The blank SCLLs and 2 × 10^{-5} M DPH solution in PBS (25:75 µL) were firstly mixed in a 96-well plate and then subjected to shaking in an orbital shaker (IKA® MS1 Minishaker, Sigma-Aldrich, Willmington, NC, USA) at 500 rpm for 30 min in the absence of light. Next, different concentrations of CPEs in 0.1 M borate buffer (100 µL) were added and shaken in the same conditions. The fluorescence polarization (P_f) was measured at 25°C using a microplate reader (Spectra Max® M5^e, Molecular Devices, LLC., Sunnyvale, CA, USA) at excitation and emission wavelengths of 358 nm and 425 nm, respectively. The P_f value was calculated according to the following equation:

$$P_f = \left(\frac{I_{||} - GI_{\perp}}{I_{||} + GI_{\perp}}\right) \quad (4)$$

where $I_{||}$ and $I_{\perp}$ are the fluorescence intensities of the emitted light polarized parallel and perpendicular to the excited vertical light, respectively. G is an instrumental correction factor grating correction coefficient[32,33].

In addition, the increase in SCLL membrane fluidity was calculated as follows:

$$\text{Increase in SCLL fluidity} = \left(\frac{P_{f,control} - P_{f,sample}}{P_{f,control}}\right) \text{ x } 100 \quad (5)$$

where $P_{f,control}$ was obtained from DPH-SCLL incubated with plain 0.1 M borate buffer.

For determination of the effect of ethanol concentrations on SCLL fluidity, additional two fluorescent probes, TMA-DPH and ANS, at concentrations of 1 × 10^{-5} and 6 × 10^{-3} M, respectively, were incubated with blank SCLL in the same procedure as the DPH probe. The determination of SCLL fluidity was performed on excitation and emission wavelengths of 365 nm and 430 nm for TMA-DPH, and 337 nm and 480 nm for ANS.

1.2.9. Calculation of effective concentration for promoting 10% FL leakage ($EC_{10,\ leakage}$) *and 10% increase in SCLL fluidity* ($EC_{10,\ fluidity}$) *of each CPE*

$EC_{10,\ leakage}$ and $EC_{10,\ fluidity}$ of each CPE was calculated by interpolation from the FL-leakage or SCLL fluidity-concentration profile to estimate the effectiveness of each CPE to act on the SCLLs. In this study, 10% response was selected because most CPEs, within the tested concentrations range, could promote the FL leakage as well as the SCLL fluidity. The relationship between $EC_{10,\ leakage}$ or $EC_{10,\ fluidity}$ and log $K_{o/w}$, obtained from ChemBioDraw Ultra 12.0 software, of each CPE as well as the hydrophile-lipophile balance (HLB) of surfactants was also investigated.

1.2.10. Statistics

Data were expressed as the mean ± standard error (S.E.). The differences among the obtained data were analyzed using unpaired *t*-test. The differences were considered significant when $p < 0.05$.

1.3. Results

1.3.1. Effect of ethanol on in vitro skin permeation of caffeine

In the present study, caffeine was selected as a hydrophilic model drug to evaluate the relationship between its skin permeation rate and the effect of different concentrations of ethanol on the SC lipid disruption. Figure 1-2 shows the cumulative amounts of caffeine that permeated through the excised hairless rat skin. Typical *in vitro* skin permeation profiles of caffeine (lag time and following almost steady-state profiles) were observed in all cases when using 0–100% ethanol as in the donor solution. Figure 1-3 illustrates the relationship between the increase in *ER* and the ethanol concentration in the donor solution. Figures 1-2 and 1-3 show that the skin permeation of caffeine was strongly dependent on the ethanol concentration in the caffeine solution. When the ethanol concentration increased from 0% to 50%, the caffeine flux through skin also increased. However, at 100% ethanol, caffeine permeation was rather decreased compared with the samples with 50% and 75% ethanol. The maximum skin permeation of caffeine was observed with 75% ethanol. The flux, permeability coefficient and

skin penetration-enhancement ratio (*ER*) of caffeine obtained from different concentrations of ethanol are also summarized in Table 1-2.

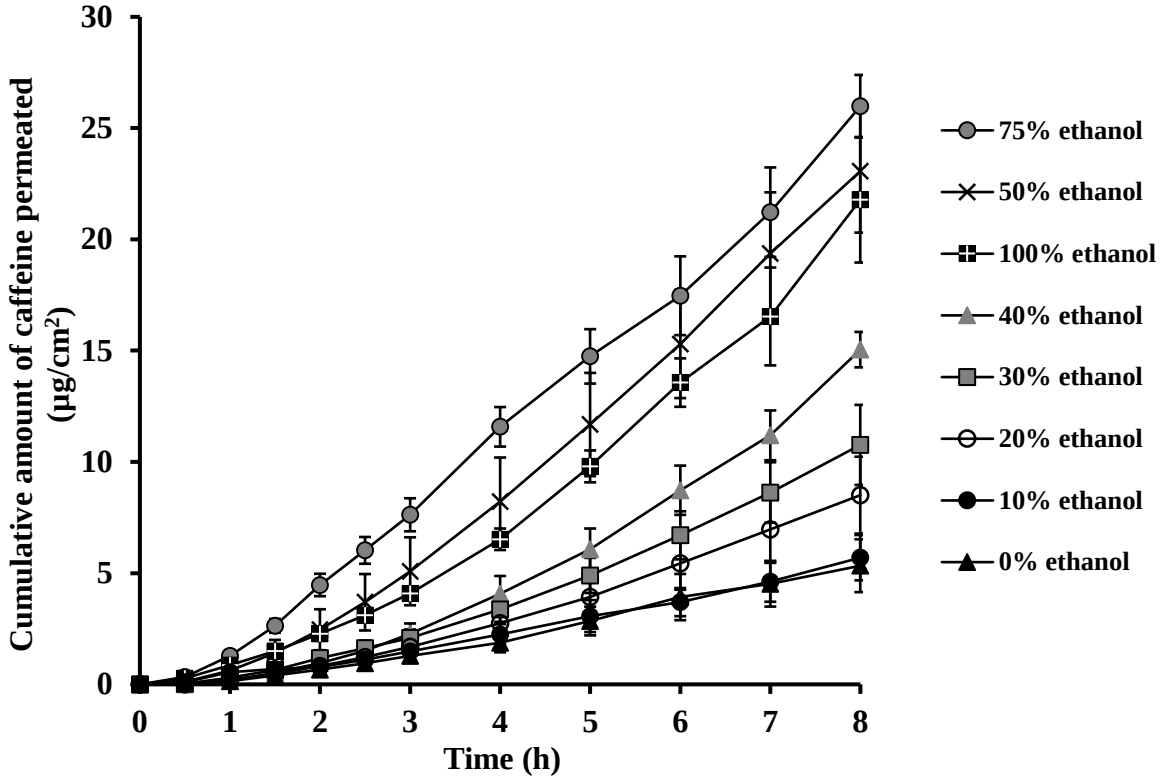

Fig. 1-2. Time course of cumulative amount of caffeine permeated through full-thickness hairless rat skin after application with different concentrations of ethanol. Each value represents the mean ± S.E. (n = 3–5).

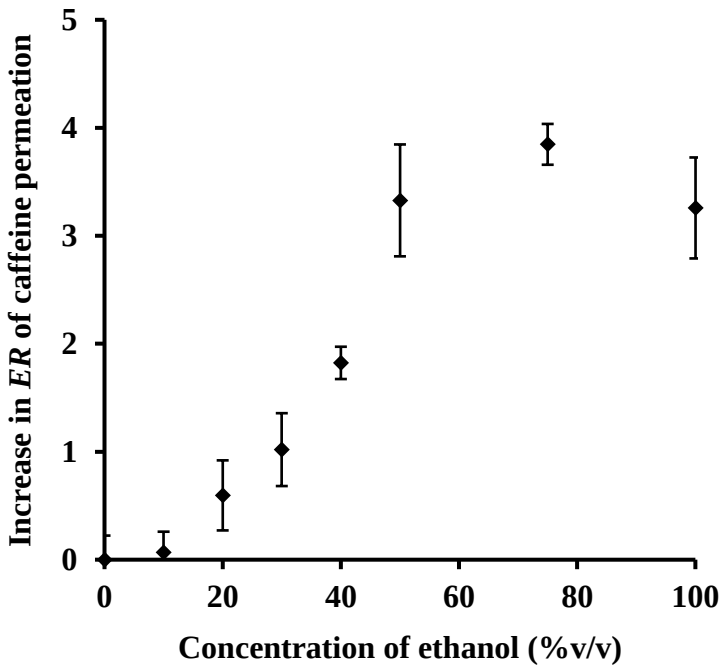

Fig. 1-3. Effect of ethanol concentration on the increase in *ER* of caffeine that permeated through full-thickness hairless rat skin over 8 h. Each value represents the mean ± S.E. (n = 3–5).

Table 1-2. Flux, permeability coefficient and *ER* of caffeine that permeated through full-thickness hairless rat skin from different concentrations of ethanol

Formulation	**Flux** ($\mu g/cm^2/h$)	**Permeability coefficient** ($x10^{-7}$ cm/s)	**Enhancement ratio** (***ER***)
0% ethanol	0.80 ± 0.18	1.12 ± 0.25	1.00 ± 0.22
10% ethanol	0.80 ± 0.15	1.11 ± 0.20	1.07 ± 0.19
20% ethanol	1.29 ± 0.27	1.79 ± 0.37	1.60 ± 0.32
30% ethanol	1.59 ± 0.26	2.21 ± 0.36	2.02 ± 0.34
40% ethanol	2.29 ± 0.12	3.18 ± 0.17	2.82 ± 0.15
50% ethanol	3.47 ± 0.36	4.81 ± 0.50	4.33 ± 0.52
75% ethanol	3.38 ± 0.24	4.69 ± 0.34	4.85 ± 0.19
100% ethanol	3.35 ± 0.37	4.65 ± 0.52	4.26 ± 0.47

1.3.2. Effect of ethanol on the skin impedance

Skin impedance has been used as an index of the skin permeation rate of drugs, especially of hydrophilic drugs, because the decrease in skin impedance is related to decreased barrier function of the skin. Therefore, skin impedance after pretreatment with different concentrations of ethanol was determined. Figure 1-4 shows the decrease in skin impedance with different concentrations of ethanol on the excised back skin of hairless rats. Ethanol treatment changed the skin impedance even at a low concentration. Ethanol solution at a concentration of 5% reduced skin impedance by about 30%, and 20–100% ethanol could reduce skin impedance about 75–80%.

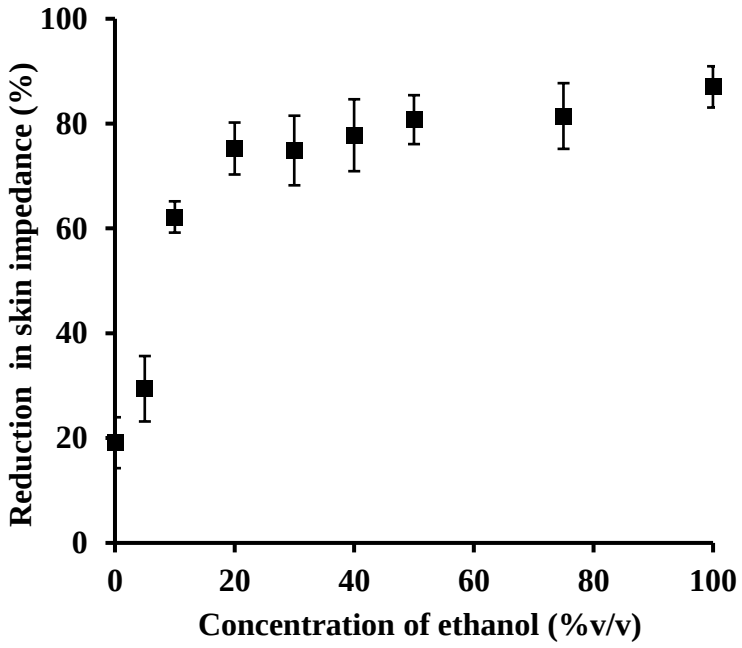

Fig. 1-4. Effect of different concentrations of ethanol on the percentage of reduction in skin impedance. Each value represents the mean ± S.E. (n = 3–5). The excised back skin from hairless rat was used.

1.3.3. SCLLs characteristics

Table 1-3 summarizes the characteristics of blank SCLLs and FL-SCLLs prepared in the present study. The vesicle size and distribution of FL-SCLLs were a little larger but narrower, respectively, than the blank SCLLs, indicating that the vesicle dispersion was homogeneous. Both the liposome formulations showed highly negative surface charge of -87.0 ± 2.3 and -99.6 ± 3.3 mV, respectively, because of the ionized fraction of fatty acids at pH 9.0. The presence of FL anions inside the SCLLs leads to higher negative surface charge. The zeta potential of both SCLL formulations indicated high electrostatic repulsion among the particles and excellent kinetic stability[34]. The entrapment of FL inside SCLLs was 1.78 ± 0.04%.

Table 1-3. Characteristics of blank SCLLs and FL entrapped in SCLLs (FL-SCLLs)

	Blank SCLLs	**FL-SCLLs**
Size (nm)	221.1 ± 8.6	282.8 ± 3.2
Polydispersity index	0.556 ± 0.017	0.215 ± 0.014
Zeta potential (mV)	-87.0 ± 2.3	-99.6 ± 3.3
Entrapment (%)	-	1.78 ± 0.04

1.3.4. Effect of ethanol on the FL leakage from SCLLs

Next, the effect of different concentrations of ethanol was tested on the disruption of SCLLs. Figure 1-5 shows the relation between the FL leakage (%) and ethanol concentration. As the ethanol concentration increased, FL leakage also increased in a concentration-dependent manner. At low ethanol concentrations (0–5% ethanol), no significant promotion was observed in FL leakage compared with the control (0.1 M borate buffer). At higher concentrations of ethanol, on the other hand, FL leakage increased proportionally with the concentration. However, no more FL leakage was observed at more than 50% ethanol.

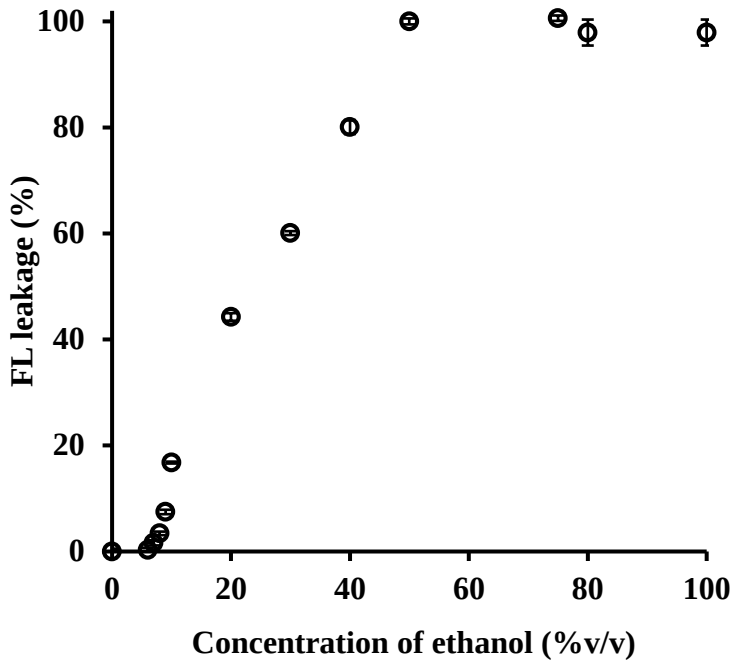

Fig. 1-5. Effect of different concentrations of ethanol on the FL leakage from SCLLs. Each value represents the mean ± S.E. (n = 3).

1.3.5. Effect of ethanol on membrane fluidity of SCLLs

Figure 1-6 shows the membrane fluidity of blank SCLLs incubated with fluorescent probes with different lipophilicities. The results with DPH and TMA-DPH as fluorescent probes showed relatively low membrane fluidity. The maximum increase was observed at 100% ethanol, which provided 37.8% and 17.9% increase in SCLL fluidity for DPH and TMA-DPH, respectively. High membrane fluidity was observed when using ANS probe at low concentrations of ethanol (0-20% ethanol).

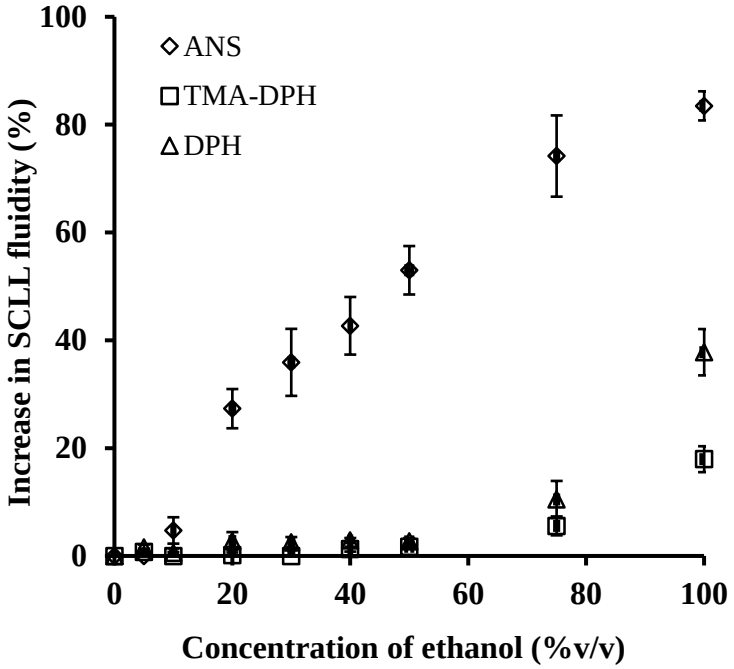

Fig. 1-6. Effect of different concentrations of ethanol on the percentage of increase in SCLL fluidity using three fluorescent probes, DPH, TMA-DPH and ANS. Each value represents the mean ± S.E. (n = 3).

1.3.6. Relationship between FL leakage and increase in ER

SCLLs were used as an SC lipid model to investigate the enhancing effect of ethanol on the skin permeation of caffeine. The correlation was evaluated between the present SCLL-based HTS data and the conventional skin penetration-enhancing profiles of caffeine. Figure 1-7a shows the relationship between FL leakage (%) from SCLLs (X-axis) and the increase in *ER* of the cumulative amount of caffeine permeated through skin over 8 h (Y-axis). The coefficient of determination (R^2) of this relationship was 0.888. The obtained profile was concave relative to the Y-axis, indicating that ethanol more markedly affected the SCLL disruption than the skin permeation of caffeine, especially at low concentrations of ethanol (0-20% ethanol). Almost linear relationship could be observed at higher concentrations of ethanol. The semi-log plot, as shown in Fig. 1-7b, shows a very high R^2 of 0.974.

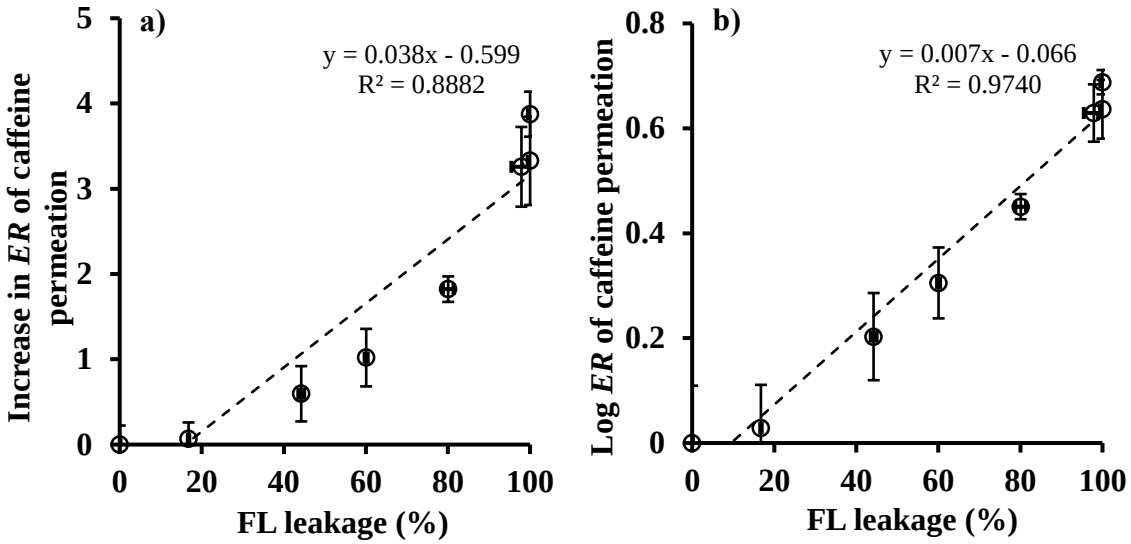

Fig. 1-7. The relationship between FL leakage and increase in *ER* (a); and log *ER* (b) of caffeine permeated over 8 h from each concentration of ethanol solution. Each value represents the mean ± S.E. (n = 3–5).

1.3.7. Relationship between SCLLs membrane fluidity and increase in ER

Figure 1-8a shows a relationship between SCLL membrane fluidity and the increase in the *ER*. The data from 100% ethanol were not included in this correlation, because the reduction in the *ER* might be exceptional, with such a high concentration of ethanol having a reversed effect on the skin permeation of caffeine. The linear relationship could be obtained in SCLL membrane fluidity measured using the ANS probe with a R^2 of 0.899, whereas DPH and TMA-DPH showed poorer correlations (R^2 of DPH and TMA-DPH; 0.638 and 0.748, respectively). A higher correlation in the data using ANS probe was obtained in the semi-log plot as shown in Fig. 1-8b, similar to Fig. 1-7b.

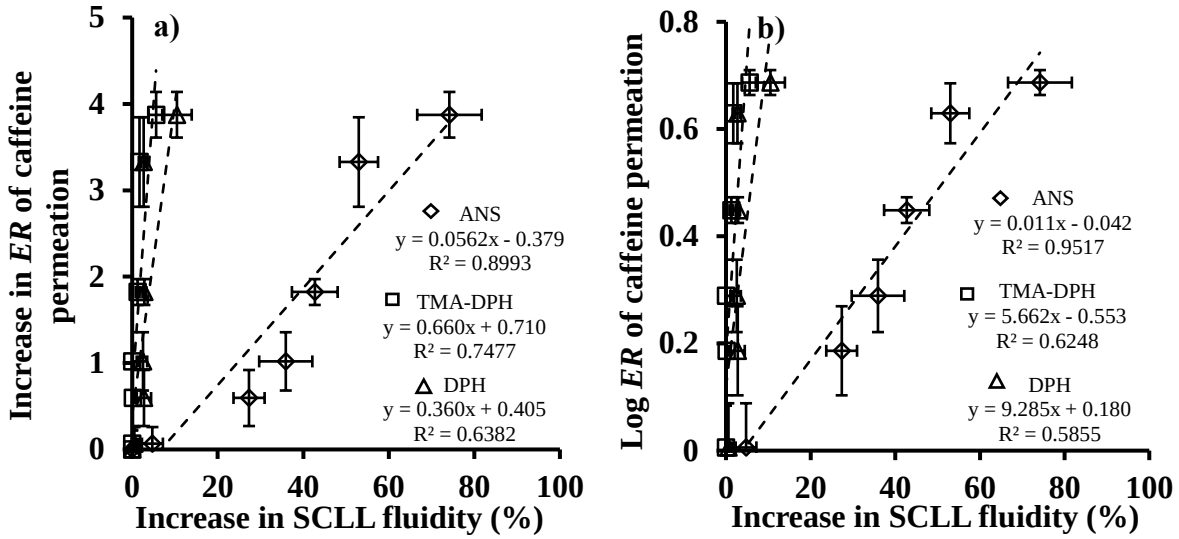

Fig. 1-8. The relationship between percentage of increase in SCLL fluidity using various fluorescent probes and increase in *ER* (a) and log *ER* (b) of caffeine permeated over 8 h from each concentration of ethanol solution. Each value represents the mean ± S.E. (n = 3–5). The data from 100% ethanol was excluded in this figure.

1.3.8. Relationship between reduction in skin impedance and increase in ER

Figure 1-9 shows a relation between reduction in skin impedance and increase in *ER*. No good relationships were observed; the R^2 was 0.456 between the increase in *ER* at 8 h and skin impedance reduction, although such skin impedance was reported to be correlated with many skin permeation data of drugs.

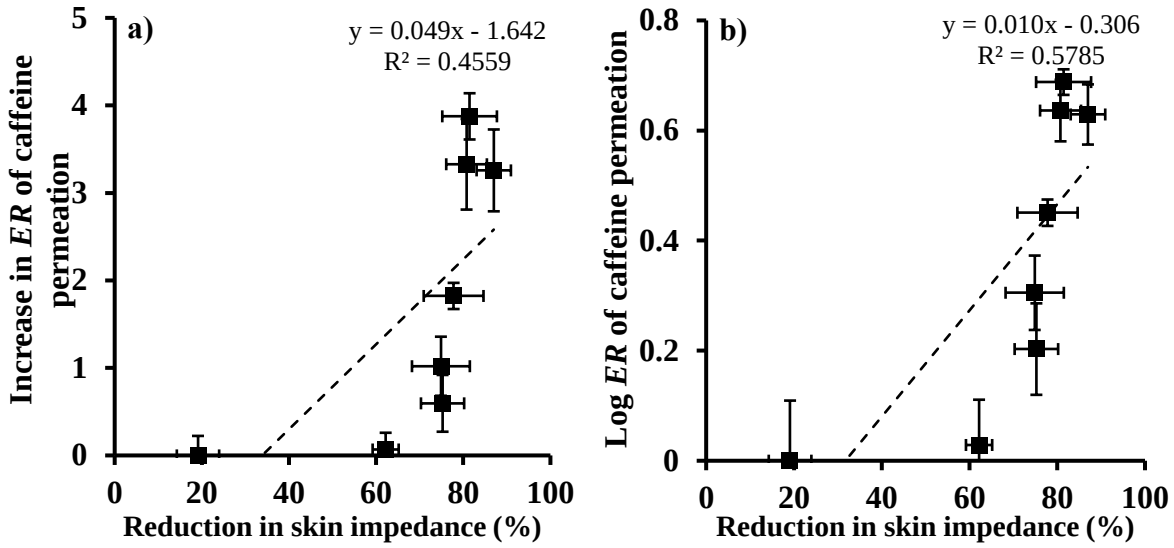

Fig. 1-9. The relationship between reduction in skin impedance and increase in *ER* (a) and log *ER* (b) of caffeine permeated over 8 h from each concentration of ethanol solution. Each value represents the mean ± S.E. (n = 3–5).

1.3.9. HTS of various types and concentrations of CPEs on FL leakage from SCLLs

FL leakage from SCLLs with the addition of different types of CPEs is shown as a function of their concentrations in Fig. 1-10. For lipophilic and amphiphilic CPEs, lower concentrations were used for evaluation compared with hydrophilic CPEs, as shown in Fig. 1-10a and b, respectively, because of their limited solubility in 0.1 M borate buffer, which was used as a dispersion medium for SCLLs. Most CPEs promoted FL leakage from SCLLs in a concentration-dependent manner except for ethyl oleate and cetylpyridinium chloride, which had no promoting effect on the FL leakage. The concentration profiles of FL leakage from different CPEs could be classified into two types, as shown in Fig. 1-11. Type I (Fig. 1-11a) showed a linear relationship between the FL leakage and CPE concentration, whereas type II (Fig. 1-11b) showed a concave downward profile, which indicated the limit level for the disruption of SCLLs. In both types, the author sometimes observed an intercept of the profile, in which the FL leakage was not promoted at lower concentrations than the X-intercept.

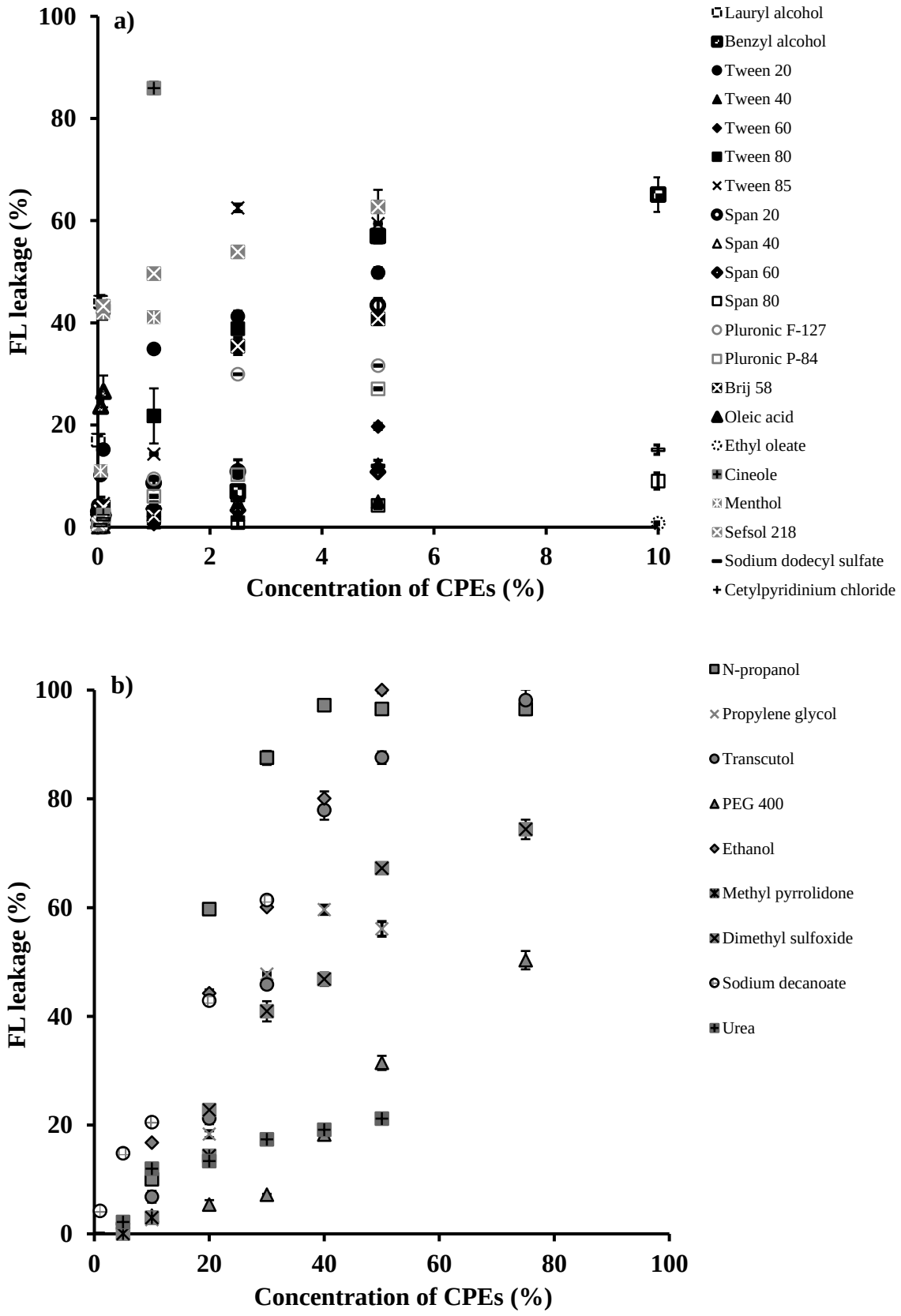

Fig. 1-10. Relationship between FL leakage from SCLLs and CPE concentration; (a) lipophilic and amphiphilic CPEs, (b) hydrophilic CPEs. Each value represents the mean ± S.E. (n = 3).

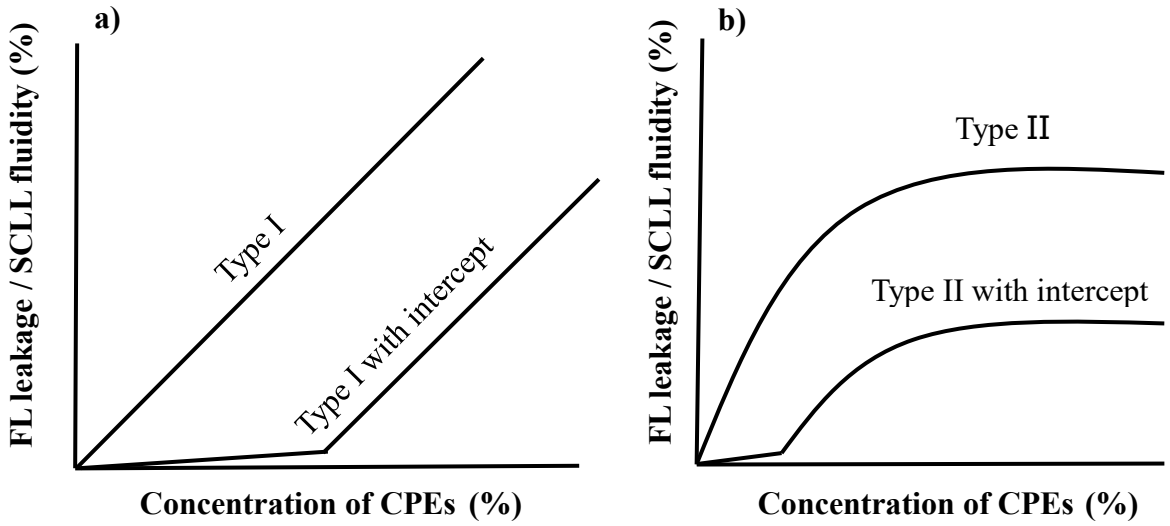

Fig. 1-11. Schematic diagram of the relationship between FL leakage and CPE concentration; (a) linear relationship (with intercept), (b) concave downward relationship (with intercept).

The $EC_{10,\ leakage}$ of each CPE is shown in Table 1-4, lipophilic CPEs were observed to provide lower $EC_{10,\ leakage}$ than hydrophilic CPEs, as shown in the plots between log $K_{o/w}$ and $EC_{10,\ leakage}$ (Fig. 1-12a). In addition, when comparing amphiphilic CPEs, the more hydrophilic surfactants showing higher HLB tended to provide lower $EC_{10,\ leakage}$ (Fig.1-12b).

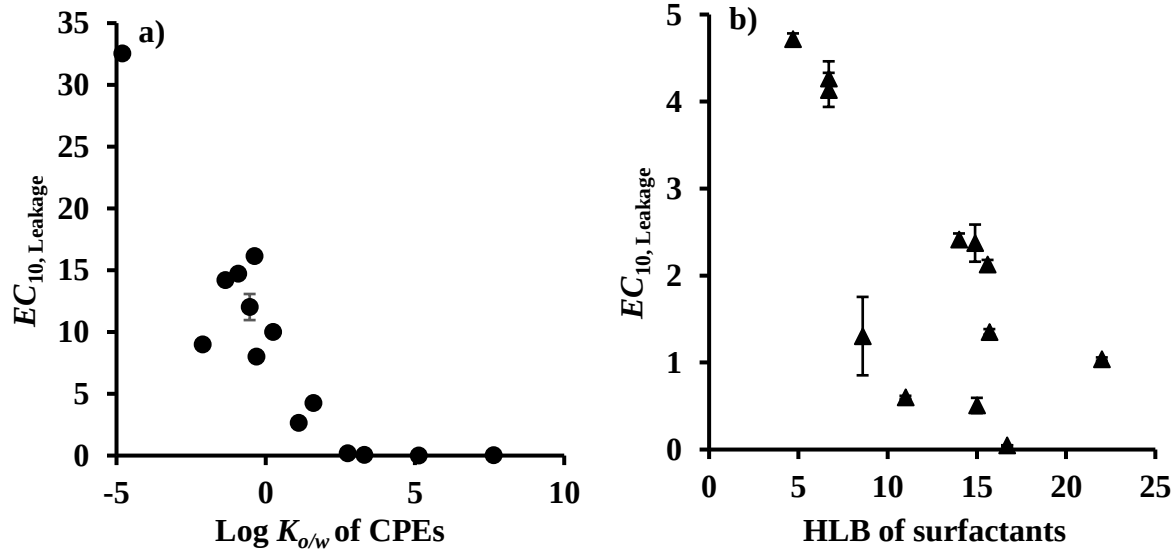

Fig. 1-12. Relationship between $EC_{10,\ leakage}$ and log $K_{o/w}$ (a) and HLB (b) of CPEs. Each plot represents a single CPE.

Table 1-4. EC_{10} value calculated from FL leakage and SCLL fluidity-concentration profile

CPEs	EC_{10} (mean ± S.E.)	
	FL leakage	**SCLL fluidity**
Lauryl alcohol	0.006 ± 0.000	>0.1%
Oleic acid	0.024 ± 0.001	0.047 ± 0.001
l-Menthol	0.047 ± 0.003	0.304 ± 0.048
Tween 20	0.048 ± 0.001	0.189 ± 0.019
Sefsol 218	0.061 ± 0.000	0.236 ± 0.010
1,8-Cineol	0.179 ± 0.027	>1%
Tween 80	0.507 ± 0.087	0.066 ± 0.004
Tween 85	0.599 ± 0.018	0.065 ± 0.002
Pluronic F-127	1.040 ± 0.019	1.331 ± 0.027
Span 20	1.304 ± 0.451	0.081 ± 0.005
Brij 58	1.352 ± 0.032	0.166 ± 0.012
Tween 40	2.127 ± 0.052	0.096 ± 0.004
Tween 60	2.372 ± 0.214	0.083 ± 0.004
Pluronic P-84	2.415 ± 0.069	2.372 ±0.172
Benzyl alcohol	2.650 ± 0.026	7.310 ± 0.012
Sodium decanoate	3.190 ± 0.117	2.950 ± 0.046
Sodium dodecyl sulfate	4.259 ± 0.037	0.283 ± 0.014
Span 40	4.266 ± 0.197	0.324 ± 0.048
Span 60	4.718 ± 0.065	0.274 ± 0.042
Ethanol	8.011 ± 0.075	67.160 ± 2.318
Urea	8.990 ± 0.039	>50%
n-Propanol	10.001 ± 0.038	44.533 ± 1.023
Transcutol	12.021 ± 1.056	>75%
Dimethyl sulfoxide	14.189 ± 0.183	>75%
Propylene glycol	14.725 ± 0.211	>75%
1-Methyl-2-pyrrolidone	16.130 ± 0.396	>20%
PEG 400	32.548 ± 0.297	>75%
Span 80	> 5%	0.048 ± 0.004
Ethyl oleate	> 0.1%	0.051 ± 0.002
Cetylpyridinium chloride	> 5%	> 5%

1.3.10. HTS of various types and concentrations of CPEs on SCLL fluidity

The relationship between fluidity of SCLLs and different concentrations of CPEs is shown in Fig. 1-13a and b for lipophilic and amphiphilic CPEs, and hydrophilic CPEs, respectively. A concentration-dependent pattern similar to the FL leakage profile was observed, unless type II with an intercept could not be observed. Most CPEs promoted the fluidity of SCLLs similar to the type II profile. The $EC_{10,\ fluidity}$ of each CPE is shown in Table 1-4. However, several CPEs promoted relatively low SCLL fluidity (less than 10%) within the concentrations used in this study; *e.g*. cetylpyridinium chloride, propylene glycol, Transcutol, urea, dimethyl sulfoxide, PEG 400, lauryl alcohol and 1,8-cineol. Among the CPEs, lipophilic CPEs provided lower $EC_{10,\ fluidity}$ in comparison with hydrophilic CPEs. For amphiphilic CPEs, no clear relationship was found between the HLB and $EC_{10,\ fluidity}$ value (data not shown).

1.3.11. The relationship between fluidity and FL leakage from SCLLs

Figure 1-14a shows the relationships between fluidity and FL leakage from SCLLs for various types of CPEs. According to the similarity in the profile patterns, the tested CPEs were categorized into 5 groups (A-E) as shown in Fig. 1-14b. Category A contains CPEs that promoted similar degree of FL leakage and the fluidity of SCLLs. The profile of this category showed a linear correlation between FL leakage and fluidity of SCLLs. Category B includes CPEs that promoted high fluidity but low FL leakage, the plots parallel to the Y-axis was observed. Similarly, CPEs in category C promoted high fluidity of SCLLs, however, at higher concentrations, higher FL leakage was then observed. The plots of this category were first parallel to the Y-axis, after a marked increase in fluidity, the curve bended toward the X-axis. Therefore, two slopes could be found in this category's profile. Category D includes CPEs that promoted high FL leakage but low fluidity. The plot in this category CPEs was almost parallel to X-axis. Finally, category E contains CPEs that could not be classified into any of the previously defined categories, then the CPEs that exhibited scattering profile were classified in this category.

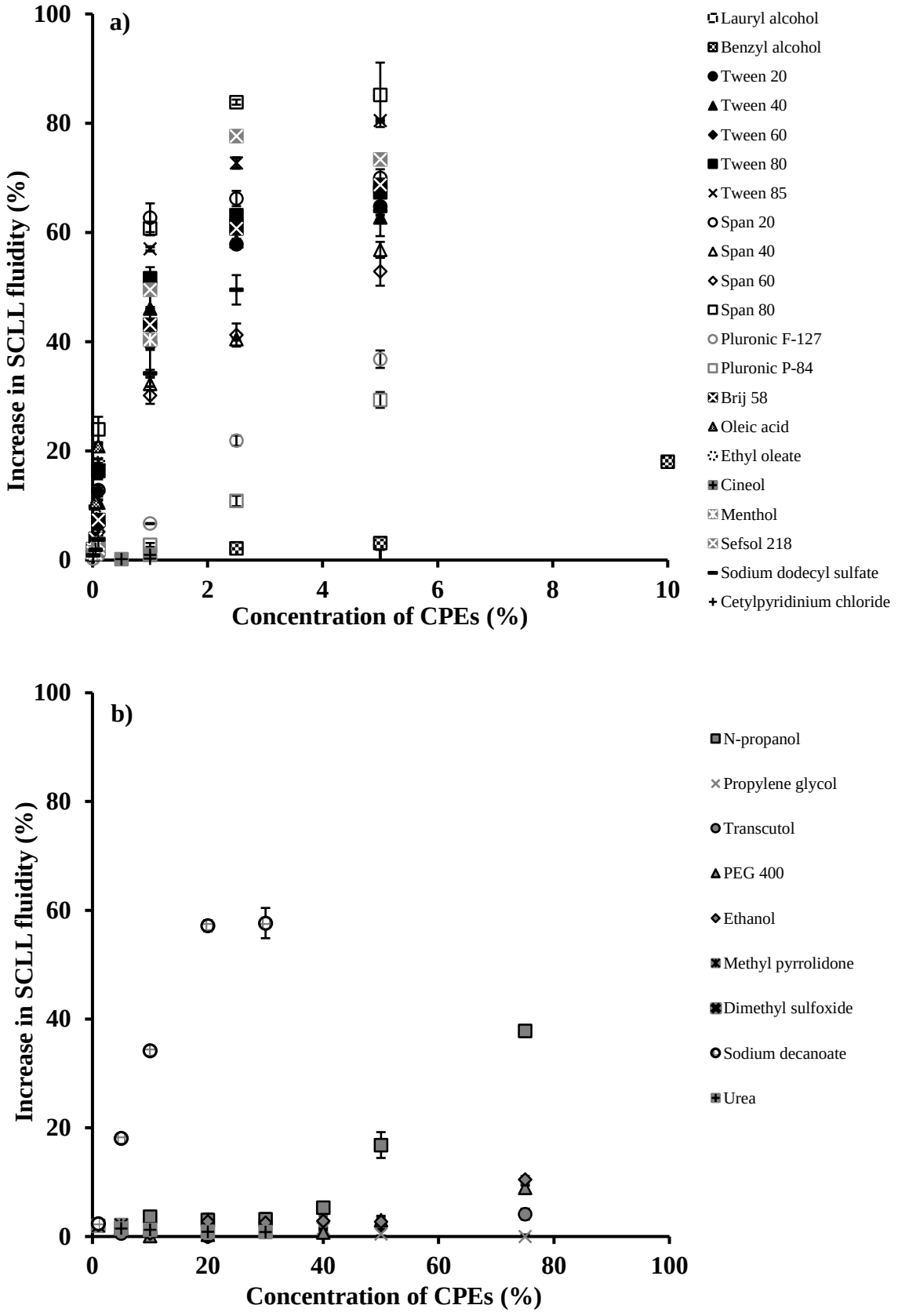

Fig. 1-13. Relationship between fluidity of SCLLs and CPE concentration; (a) lipophilic and amphiphilic CPEs, (b) hydrophilic CPEs. Each value represents the mean ± S.E. (n = 3).

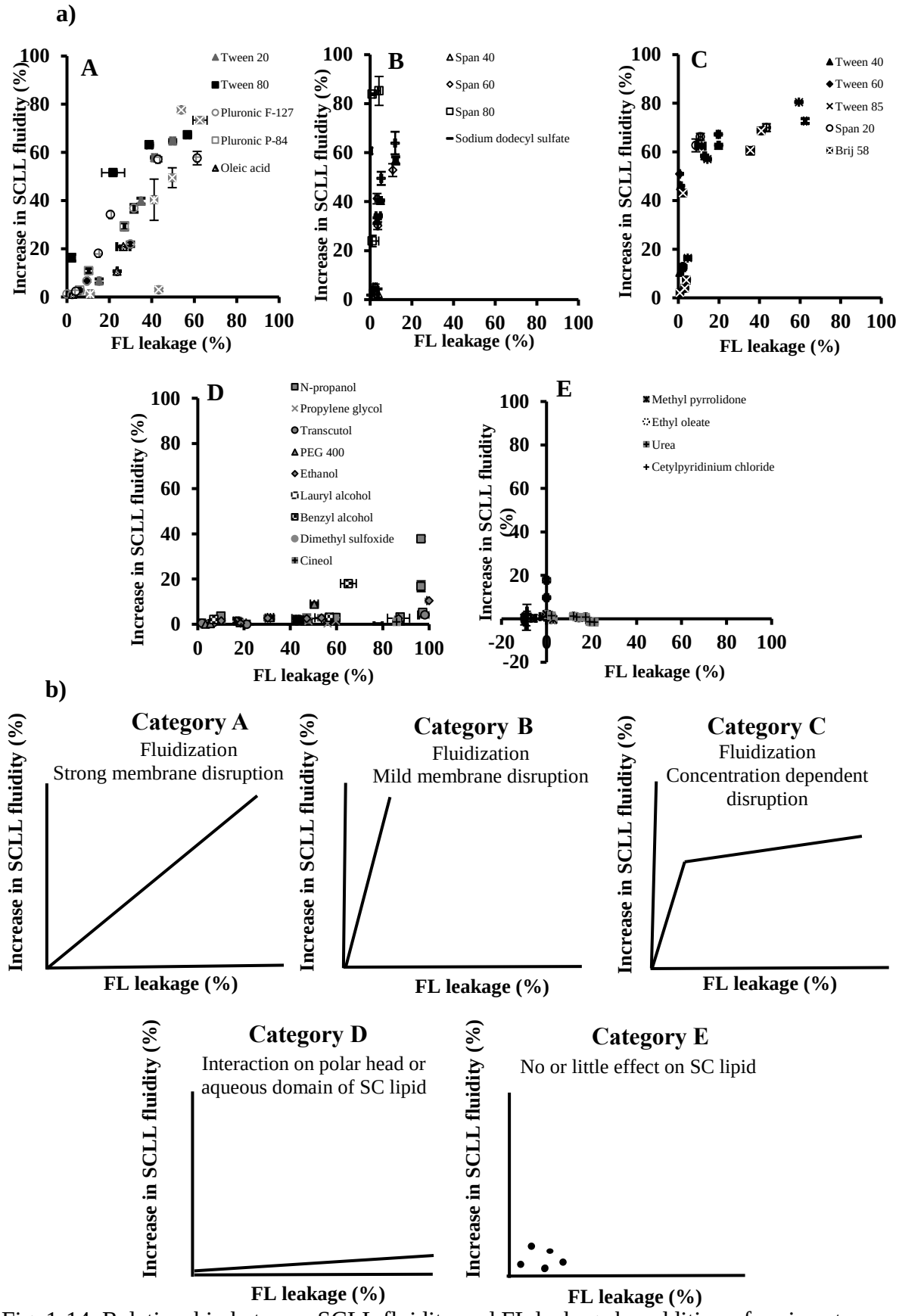

Fig. 1-14. Relationship between SCLL fluidity and FL leakage by addition of various types of CPEs and their categorization, (a) observed data, (b) categorization.

1.4. Discussion

Use of CPEs represents an easy and well-established approach to enhance the skin penetration of drugs. One of the mechanisms for the effects of CPEs can be explained by the lipid-protein-partitioning (LPP) theory[35], in which CPEs act by disrupting the highly ordered lamellar structure of SC lipids, interacting with intracellular proteins to promote drug permeation through the corneocyte layer, and increasing the partitioning of drugs into the SC. SCLLs exhibit similar characteristics to the SC intercellular lipids without the proteins associated with the SC. Thus, SCLLs were utilized in the present study as a model membrane to assess the interaction of various CPEs specifically on the SC lipid region.

In the present study, the SCLLs which comprised similar lipid composition to the intercellular lipids were prepared. This SCLL vesicle was obtained as unilamellar by an extrusion method. This SCLL morphology can be more quantitatively characterized with regards to lipid concentration, surface area and volume as well as a higher stability than multilamellar vesicles which present similar multilamellar structure to the SC lipids. Borate buffer pH 9.0 was used to prepare SCLLs as well as to dissolve CPEs, regardless of the skin pH of 4-7, to maintain the stability of SCLL vesicle derived from ionized moieties of cholesterol sulfate and free fatty acids in this pH[30].

A fluorescent hydrophilic marker, FL, was entrapped in SCLLs in order to monitor the degree of its membrane rupture by CPEs. Furthermore, fluidity of the SCLL membrane was also measured using various lipophilicities of probes in an HTS manner. These experiments were compared with conventional methods for determination of skin penetration-enhancing effect of chemicals: *in vitro* permeation and impedance studies using hairless rat skin. A well-known CPE contained in many topical and transdermal formulations, ethanol, was used in the first step to test for the suitability of this HTS approach.

The present skin permeation experiments of caffeine were conducted in asymmetric conditions in order to determine the penetration-enhancing effect of ethanol. The increase in *ER* by ethanol was found to be concentration dependent. A similar ethanol concentration-dependent effect was observed when using indomethacin in a previous study[36]. The highest permeation of caffeine was not observed at the highest ethanol concentration, because highly concentrated ethanol dehydrates the skin membrane and reduces the skin permeation of drugs[37]. Previous study also found that the skin permeability of hydrophilic drugs was

increased but inversely decreased by low and high concentration of ethanol, respectively[38]. In addition, X-ray diffraction data confirmed that low concentrations of ethanol disturbed the short lamellar structure of SC lipids, but the high concentration caused an aligned structure[39].

Skin impedance has been reported to well correlate with drug permeability through skin[8,38]. Then, back skin impedance was determined to increase the sensitivity of ethanol effect on the skin impedance. Ethanol could reduce the skin impedance and clearly alter the flux of low molecular weight ions through the skin[38]. Nevertheless, the obtained results in this study did not show linearity between the reduction in skin impedance and the increase in *ER*. This is because low concentrations of ethanol could greatly reduce the skin impedance but higher concentrations remained stable. Therefore, the reduction in skin impedance by ethanol might not be a quantitative indicator for the skin penetration-enhancing effect in this case.

FL leakage was observed from SCLL at low (≥5%) to high (~100%) concentrations of ethanol and the degree was ethanol-concentration dependent, suggesting that the disruption effect on the SCLL membrane was closely related to ethanol concentration. Ethanol has been reported as a markedly effective skin penetration enhancer by various mechanisms; increase in drug solubility, improvement in drug partitioning into the SC, modification of thermodynamic activity of drugs, solvent (ethanol) drag effect across the skin, fluidization and extraction of SC lipids, and the structure modification of SC keratin[37,40]. SCLLs used in the present experiment are model SC lipids with a lack of cellular proteins such as keratin[10]. Therefore, the present SCLL leakage results might not be totally predictive for all mechanisms associated with the skin penetration-enhancing effects of ethanol.

SCLLs mimic intercellular lipids in SC where CPEs act. Then, three different fluorescent probes; DPH, TMA-DPH and ANS, were used to determine the SCLL membrane fluidity in order to better understand the effect of ethanol on the lipid packing. High fluidity in the SCLL membrane represents a high degree of lipid molecule disorganization, which provides high permeability of drugs through the bilayer[41]. The effect of ethanol on the fluidity of SCLL was determined, especially in the region where each fluorescent probe was contained, as depicted in Fig. 1-15. DPH and TMA-DPH serve as markers for determination of molecular movement in the hydrophobic core and superficial surface of SCLLs[31], respectively. The effect of ethanol on the SCLL fluidity using DPH and TMA-DPH showed similar patterns. In the present study, lower ethanol concentrations could not promote SCLL fluidity and the effect was clearly found with more than 50% ethanol. On the other hand, ANS, a marker of molecular

movement on the exterior membrane surface[31)], changed the membrane fluidity even at low ethanol concentrations, and good linearity was observed between SCLL fluidity and ethanol concentration. These results using three fluorescent probes provided a possible effect of ethanol on the SCLL membranes. Thus, ethanol mainly disrupted the polar head region at the outside of liposome membrane similar in a previous report[42)]. Good correlations were obtained especially in the FL leakage and SCLL fluidity detected using the ANS probe, indicating that SCLLs could be an optional model to investigate the skin penetration-enhancing effects of CPEs as well as their mode of actions.

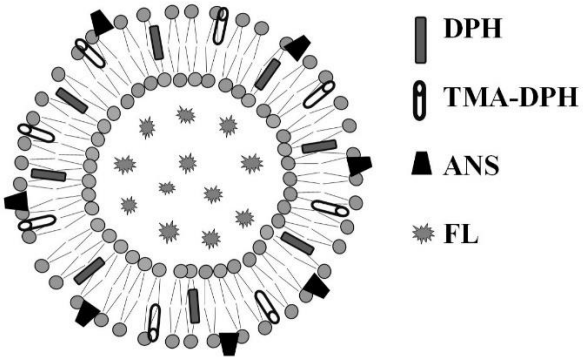

Fig. 1-15. Location of three different fluorescent probes in SCLLs.

Furthermore, the effect of various types and concentrations of CPEs on the FL leakage and SCLL membrane fluidity measured using a DPH probe, which serves as a marker for molecular movement in the hydrophobic region of SCLL[43)], was systematically evaluated. Lower $EC_{10,\ leakage}$ and $EC_{10,\ fluidity}$ were observed from lipophilic CPEs than hydrophilic CPEs. It has been discussed previously that more lipophilic compounds penetrate more easily into the SCLL membrane and more effectively reduce the barrier function of the membrane[22)]. However, several CPEs slightly promoted leakage and fluidity, thus calculation of the exact EC_{10} value was difficult.

From the relationship between SCLL fluidity and FL leakage, 5 categories of CPEs could be observed. Category A contained several non-ionic surfactants; *e.g*. Tween 20 and 80, Pluronic F-127 and P-84, fatty acids and its derivatives such as oleic acid, sodium decanoate, Sefsol 218 as well as *l*-menthol. Fatty acids such as oleic acid was reported to disturb the packing of lipids and thereby increase the fluidity of lipids as well as form a permeable defect within the SC lipids[44,45)].

Category B contained Span 40, 60 and 80, and sodium dodecyl sulfate. This group comprised mainly hydrophobic non-ionic surfactants (HLB 4-7) and anionic surfactants (HLB 40). These CPEs may insert into the hydrophobic region of SCLLs to promote higher membrane fluidity but not strong enough to promote the leakage from the SCLLs.

Most non-ionic surfactants such as Tween 40, 60, 85, Span 20 and Brij 58 were classified into category C. These CPEs showed a similar action to the CPEs in category B, by fluidization of SCLL. In addition, high leakage was also observed at a higher concentration. This phenomenon might be due to the insertion of these non-ionic surfactant molecules in the hydrophobic area of SCLL. At a higher concentration, the degree of fluidization is strong enough to disturb the SCLLs structure consequently allowing FL to leak outside.

Non-ionic surfactants could be categorized into either category A, B or C. These findings are in good agreement with the skin penetration-enhancing mechanisms reported that surfactants may intercalate into lipid bilayers of SC, resulting to increase fluidity of intercellular SC lipids which finally solubilize and extract the lipid components[46]. The effect of surfactants on the SCLLs could vary from mild to strong as could be observed from each category. However, the surfactant effects on the keratin filament could not be observed using this model membrane.

The following CPEs; *n*-propanol, propylene glycol, Transcutol, PEG 400, ethanol, lauryl alcohol, benzyl alcohol, dimethyl sulfoxide and 1,8-cineol were classified in category D. Alcohols and glycols as classified under this category were reported to interact the aqueous domain of the lipid bilayers which increase the drug solubility in the skin[47]. In addition, ethanol has been reported to extract and fluidize SC lipids[48-50]. Dimethyl sulfoxide has been shown to change keratin conformation and interact with SC lipids[51,52]. However, the interactions of these CPEs with SC lipids were mainly on the polar head region[39,51,53]. Therefore, low fluidity in the hydrophobic chain of SCLL lipids was observed in the present study.

1-Methyl-2-pyrrolidone, ethyl oleate, urea and cetylpyridinium chloride were classified in category E, in which the profile could not be categorized in any previous categories. The skin penetration-enhancing effect of urea and its derivatives are from keratolytic and moisturizing effects; cationic surfactants act on the skin proteins; whereas pyrrolidone derivatives act on the drug partitioning into SC to alter the solvent nature of SC[54,55]. In addition, ethyl oleate is highly lipophilic (log $K_{o/w}$ 6.89). Its low solubility in SCLL dispersion medium

might be a reason for low disruption effect on the SCLLs since ethyl oleate could not be exposed and penetrated into the SCLLs membrane. Thus, these reasons might support category E of exhibiting no trend in the SCLL fluidity and FL leakage plot.

The modes of action for each category of CPEs could be proposed as follows: CPEs in the categories A, B and C might mainly act by fluidization of SC lipids, although the degree of fluidization is different among categories. The degree of fluidization of CPEs in category A is strong, so that they could disrupt the SC lipids and promote the diffusion of drugs through the SC lipids, which is evident from high FL leakage profile. Category B provides mild degree of fluidization, therefore they could not promote the diffusion of drugs through SC lipids. Category C is similar to category B, but the degree of fluidization is strong enough to disrupt the SC structure at their higher concentrations. On the other hand, category D might act at the lipid polar head group or at the aqueous region between the lipid head groups. Finally, category E did not manifest any trend, thus its mechanism of action cannot be identified using the present method on the SCLL model.

1.5. Chapter conclusion

The present HTS approach using SCLLs could be a promising model to determine the effect of various kinds of CPEs on the skin permeability of drugs, because a good correlation was obtained from SCLL-based experiments and skin permeation study using ethanol as a model CPE. The ease of handling of the various fluorescent probes could also identify the possible mechanisms of action of CPEs for enhancing the skin permeation of drugs. The present HTS approach provided benefits over other conventional skin penetration and skin impedance studies, *i.e.*, small quantity of sample is required, and rapid, simultaneous and simple determination can be performed using a fluorescent microplate reader and can avoid the use of animals which impractical in ethical issues. The presently evaluated approach exhibited good feasibility to test new CPE candidates in the skin formulation development.

Chapter 2

Development of penetration enhancing vesicular carriers based on the skin penetration-enhancing properties of materials

2.1. Introduction

Vesicular carriers including liposomes and niosomes have been received high attention in the field of skin drug delivery during this few decades due to their ability to entrap and act as chemical carriers to enhance the skin penetration of both hydrophilic and lipophilic molecules[56-58]. The main compositions of liposome and niosome formulations are phospholipids and non-ionic surfactants, respectively, which can spontaneously form the structure of closed bilayers vesicles as they confront with water[7]. The mechanisms to enhance the skin penetration of drugs using vesicular carriers have been proposed as 1) free drug operation, 2) intact vesicular penetration, 3) vesicle adsorption to and/or fusion with the SC and 4) penetration enhancing effect[59,60]. However, conflicting results on these mechanisms have been found in spite of much efforts made by many researchers.

One of the well-accepted mechanisms for the skin penetration-enhancement effect of vesicles is the penetration of the amphiphilic components (phospholipids and non-ionic surfactants) from the vesicles to skin and perturbation of the packing of SC lipids[59-62]. From this reason, the amphiphilic composition of vesicles is an important optimization factor that should be considered to enhance the skin penetration of drugs. Several studies have focused on the vesicular characteristics, for examples, morphology, vesicular size, surface charge, entrapment efficiency, transition temperature, or elasticity as factors to optimize and enhance the skin penetration of drugs[63-65]. Other studies have developed novel classes of vesicular carriers to obtain high penetration enhancing effect, by addition of edge activators or CPEs into the classical liposomes and niosomes[63,66-68]. However, very limited studies have considered the effect of the amphiphilic compositions as an optimization factor to enhance the skin permeation of drugs. Understanding the effect of vesicle compositions on their penetration-enhancing ability could enable researchers to develop vesicles that intended to improve the skin penetration of drugs.

This study was aimed to develop a novel approach to formulate penetration-enhancement vesicles. This approach was based on the selection of the vesicular carrier's composition by *in vitro* skin permeation screening to assess the suitable compositions with high skin penetration-enhancing effect for a hydrophilic model drug; caffeine. Liposomes and niosomes were prepared from their main compositions; phospholipids and non-ionic surfactants, respectively. The skin penetration-enhancing property of these vesicles was then evaluated and compared to their composition dispersions. In addition, two kinds of experiments were done to clarify the possible mechanism of liposomes as follows: the excised skin was pretreated for 1 h with caffeine-free phospholipid dispersions and liposomes, and caffeine solution was added to determine its skin permeation. Separately, caffeine permeation experiments were done using physical mixture of blank liposomes and caffeine solution (caffeine-spiked liposomes) and caffeine-entrapped liposomes (caffeine was entrapped only in liposomes).

2.2. Materials and methods

2.2.1. *Materials*

Phospholipids including 1,2-dilauroyl-*sn*-glycero-3-phosphocholine (DLPC), 1,2-dimyristoyl-*sn*-glycero-3-phosphocholine (DMPC), 1,2-dimyristoyl-*sn*-glycero-3-phospho-glycerol, sodium salt (DMPG), 1,2-dipalmitoyl-*sn*-glycero-3-phosphocholine (DPPC), 1,2-dipalmitoyl-*sn*-glycero-3-phosphoglycerol, sodium salt (DPPG), 1,2-distearoyl-*sn*-glycero-3-phosphocholine (DSPC), 1,2-distearoyl-*sn*-glycero-3-phosphoglycerol, sodium salt (DSPG), 1,2-dioleoyl-*sn*-glycero-3-phosphocholine (DOPC) and 1,2-dioleoyl-*sn*-glycero-3-phospho glycerol, sodium salt (DOPG) were purchased from NOF Corporation (Tokyo, Japan). 1,2-Dilauroyl-*sn*-glycero-3-phosphoglycerol, sodium salt (DLPG) was obtained from Olbracht Serdary Research Laboratories (Toronto, ON, Canada). Tween 20, 40, 60, 80, 85 and Span 20, 40, 60, 80 were obtained from Tokyo Chemical Industry Co., Ltd. (Tokyo, Japan). Brij 35 was obtained from MP Biomedical, LLC (Illkirch, France). Cholesterol was purchased from Sigma-Aldrich (St. Louis, MO, USA). Caffeine, chloroform, methanol and ethanol were purchased from Wako Pure Chemicals Industries, Ltd. (Osaka, Japan). Propylene glycol was purchased from Kanto Chemical Co., Inc., (Tokyo, Japan). These reagents were used without further purification.

2.2.2. Determination of skin penetration-enhancing effect of phospholipid and non-ionic surfactant dispersions

The skin penetration-enhancing effect of different types of phospholipid and non-ionic surfactant dispersions were determined using a diffusion cell array system (Ikeda Scientific Co., Ltd., Tokyo, Japan). This system is comprised of 12 wells wherein the donor compartment is above the receiver chamber with the excised skin sandwiched between them. Effective permeation area and receiver volume for each well are 0.785 cm^2 and 1.36 mL, respectively. The study was performed using excised abdominal skin from hairless rat after removing subcutaneous fat as described in sections 1.2.2. and 1.2.3. The skin was excised and cut into two pieces of 3 x 4 cm size from the middle line of rat abdomen and set on the diffusion cell array system as shown in Fig. 2-1. At first, 1.0 and 1.36 mL PBS were added in the donor and receiver chamber, respectively, for 1 h for skin hydration. After that, PBS was removed from donor compartment and replaced with 200 µL of 3% w/v phospholipids/non-ionic surfactants dispersions containing caffeine in PBS at a concentration of 100 mM. The skin permeation experiment was performed at 32°C using a thermo-shaker at the rotation speed of 200 rpm and the receiver solution was stirred using a stir ball for 12 h. At the end of the permeation experiment, the receiver solution was collected to determine the amount of caffeine that permeated per unit of skin area (*Q*) by an HPLC. Caffeine solution (100 mM) in PBS was used as a control and calculated for skin penetration-enhancement ratio (*ER*) of each sample by the following equation;

$$ER = \left(\frac{Q_{sample}}{Q_{control}}\right) \quad (6)$$

where Q_{sample} and $Q_{control}$ are the cumulative amount of caffeine permeated per unit area of skin over 12 h from different phospholipids/non-ionic surfactants and control solution, respectively.

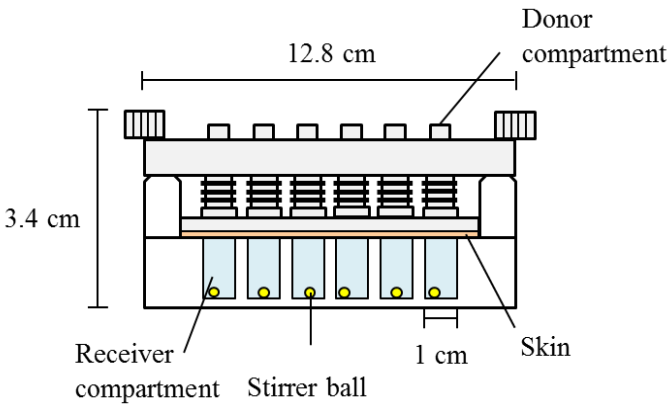

Fig. 2-1. Diffusion cell array system for *in vitro* skin permeation experiment.

2.2.3. Preparation of liposomes and niosomes

Liposomes/niosomes were prepared using phospholipids/non-ionic surfactants and cholesterol in the ratio of 4:1 w/w. The compositions were dissolved in chloroform: methanol (2:1 v/v) in a round-bottomed flask. The solvent was evaporated to form the thin film using a rotary evaporator under reduced pressure. The obtained film was purged with N_2 gas and kept overnight to remove the trace organic solvent. After that, the flask was immersed in a water bath at 90°C for annealing the thin film for 30 min, and then 100 mM caffeine in PBS solution was added to adjust phospholipids/non-ionic surfactants concentration to 3% (w/v). The thin film was hydrated for 30 min. The resulting liposomes/niosomes containing caffeine were then sonicated using a probe sonicator (VCX-750, Sonics & Materials Inc., Newtown, CT, USA) for 30 s. Next, 4 cycles of freeze-thaw process were performed by immersing the flask in liquid N_2 and in 90°C-water bath for 3 min each. The obtained liposomes were further extruded using a mini-extruder (Avanti Polar Lipids, Inc., Alabaster, AL, USA) assembled with a membrane filter (with pore sizes of 400, 200 and 100 nm, Whatman® track-etched membranes, GE Healthcare Japan, Tokyo, Japan). All final liposomes/niosomes containing caffeine were kept at room temperature and freshly used for the skin permeation experiment within the next day after preparation. In the final formulation, caffeine was contained both in the inside and outside of vesicles. These vesicle formulations were used to evaluate the caffeine permeation through skin.

Caffeine-free liposomes (blank liposomes) were also prepared with the same procedure without addition of caffeine.

2.2.4. Characterizations of liposomes and niosomes

Particle size and zeta potential

The particle size and zeta potential of liposomes and niosomes were measured after 100-fold dilution with PBS using a Zetasizer Nano ZS (Malvern Instruments Ltd., Malvern, UK). The size measurements were performed at 25°C and a scattering angle of 90°. Each individual zeta potential measurement was repeated for at least 10 readings from each sample.

Entrapment efficiency

The entrapment efficiency (*EE*) of caffeine in each vesicle formulation was determined by ultracentrifuge technique to evaluate the caffeine distribution in either inside and outside of vesicle formulations. Final vesicles suspension (400 µL) was put in a centrifuge tube and centrifuged using a micro-ultracentrifuge (Himac CS120GXII, Hitachi Koki Co., Ltd., Tokyo, Japan) to separate the vesicles pellet (entrapped drug, E_{drug}) from the supernatant (unentrapped drug, U_{drug}). The supernatant was collected and the unentrapped (free) caffeine content was determined after 10-fold dilution with ethanol followed by 10-fold with PBS. In addition, the entrapped drug content in vesicles was determined by dispersing the packed vesicle pellet with 400 µL PBS and further disrupting with 10-fold ethanol followed by dilution with 10-fold PBS. Caffeine contents were analyzed by an HPLC and the % *EE* was calculated according to the following equation.

$$\% \text{ Entrapment efficiency } (EE) = \left(\frac{E_{drug}}{E_{drug} + U_{drug}}\right) x\ 100 \qquad (7)$$

For niosomes, the *EE* was determined from the caffeine content in supernatant as shown in the following equation; where total drug (T_{drug}) was obtained from vesicles suspension disrupted with ethanol and PBS as in above mentioned procedure.

$$\% \text{ Entrapment efficiency } (EE) = \left(\frac{T_{drug} - U_{drug}}{T_{drug}}\right) x\ 100 \qquad (8)$$

Differential Scanning Calorimetry

The phase transition temperature (T_m) was determined for liposomes and niosomes membrane by a DSC Thermo plus EVO/ DSC8230, Rigaku Corporation, Japan). About 5 mg of liposome pellets obtained from the ultracentrifugation process previously described or niosomes suspension were placed in an aluminum pan. An empty pan was used as a reference. The DSC heating scan was performed at a heating rate of 5.0°C/min in a 15–80°C range.

2.2.5. In vitro skin permeation experiments of caffeine from liposomes and niosomes

Excised abdominal skin from hairless rat was mounted in a vertical-type Franz diffusion cell (effective permeation area of 1.77 cm^2 and receiver cell volume of 6.0 mL) with the SC side facing the donor cell and the dermal side facing the receiver cell. The receiver cell was filled with 6.0 mL PBS. 1.0 mL PBS was added to the donor cells for 1 h for skin hydration. Then, 400 µL of liposomes/niosomes containing caffeine at a concentration of 100 mM were replaced in the donor compartment to determine its skin permeation at 32°C over 8 h, while the receiver solution was agitated at 500 rpm using a magnetic stirrer. At predetermined times, 0.5 mL aliquots were collected and the same volume of PBS was added to keep the volume constant. The amount of caffeine permeated through skin was determined by HPLC.

2.2.6. Determination of the effect of pretreatment of caffeine-free phospholipid dispersions and liposomes on the caffeine permeation through skin

Selected caffeine-free liposomes (400 µL) prepared using phospholipids (DPPG, DLPC or DSPG) were applied onto the SC surface of skin for 1 h after the hydration period with PBS. Phospholipid dispersions (3% DPPG, DLPC or DSPG) without caffeine were also applied on skin for comparison. Then, the liposomes or phospholipid dispersion without caffeine were removed from the skin surface by washing with 1.0 mL fresh PBS for 10 times. Caffeine solution (100 mM, 400 µL) was then applied on the skin. The skin permeation experiment was conducted using vertical-type Franz diffusion cell for 8 h as previously described in the section 2.2.5.

2.2.7. Determination of the skin permeation of caffeine from the physical mixture of blank liposomes and caffeine solution (caffeine-spiked liposomes)

The caffeine-spiked liposomes containing 3% phospholipid and 100 mM caffeine was prepared by mixing the same volume of the double-concentrated liposomes (preparation method was similar to the final liposomes as above) and 200 mM caffeine. The resultant caffeine-spiked liposomes (400 µL) were used for the skin permeation experiment of caffeine using vertical-type Franz diffusion cell for 8 h as previously described in the section 2.2.5.

2.2.8. Determination of the skin permeation of caffeine from caffeine-entrapped liposomes

Caffeine-entrapped DPPG, DLPC and DSPG liposomes were obtained by ultracentrifugation separation as described previously. In the preparation process, free caffeine was totally removed and the remained caffeine-entrapped liposomes pellet was dispersed with PBS (400 µL). The skin permeation experiment using this caffeine-entrapped liposome formulation was performed and compared with the same concentration of free caffeine solution.

2.2.9. Determination of caffeine content

The concentration of caffeine was determined as described in the section 1.2.5.

2.2.10. Statistical analysis

Data were expressed as the mean ± standard error (S.E.) or standard deviation (S.D.). The differences among the obtained data were analyzed using unpaired *t*-test. The differences were considered to be significant when $p < 0.05$.

2.3. Results

2.3.1. Skin penetration-enhancing effect of phospholipid and non-ionic surfactant dispersions

The *ER* of caffeine permeation in the presence of 3% phospholipid/non-ionic surfactant dispersion in PBS against that of free caffeine solution in PBS is shown in Fig. 2-2. DSPC and DPPG dispersions significantly enhanced the skin permeation of caffeine (*ER* 1.93 and 1.57, respectively), whereas DOPG dispersion provided the lowest skin permeation of caffeine (*ER* = 0.38). While the other phospholipid dispersions had no or little skin penetration-enhancing effect against the control group. Non-ionic surfactants including Brij 30 and Span 20 dispersions showed significantly higher *ER* (7.72 and 3.53, respectively) as compared to the *ER* obtained from phospholipids dispersion. In addition, other non-ionic surfactants resulted in about 1.3-2.0 times *ER*, wherein Tween 20, 40 and 60 showed significant difference in the caffeine permeation compared to the control solution as shown in Fig. 2-3.

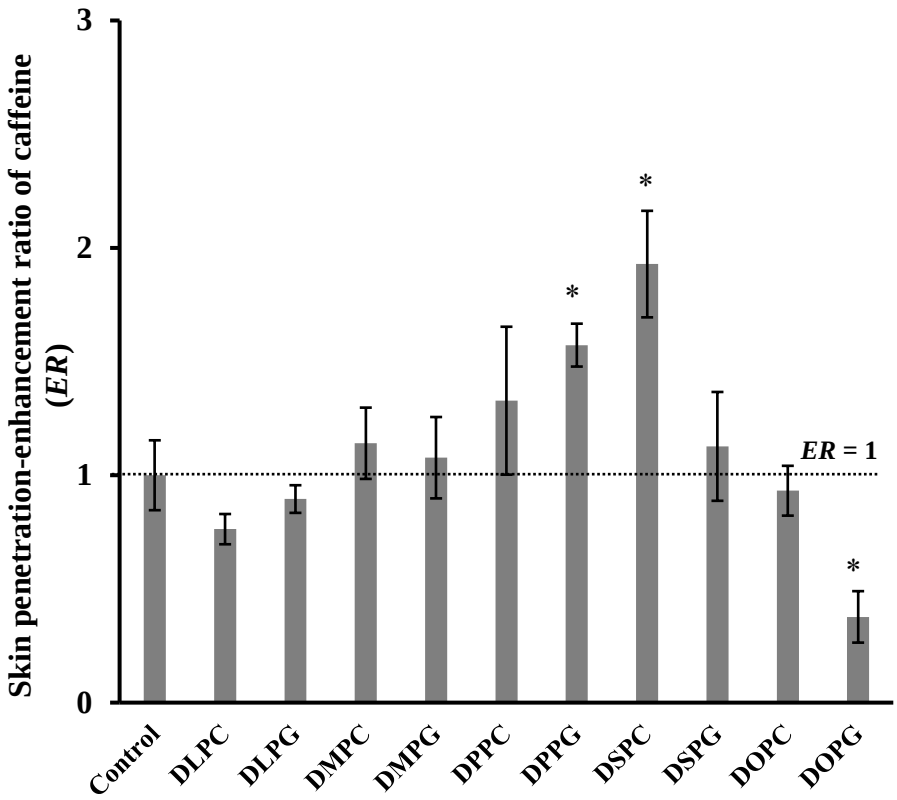

Fig. 2-2. *ER* of caffeine permeation through skin from different phospholipid dispersions. Each value represents the mean ± S.E. (n = 3–4). *: $p < 0.05$ significantly different from control.

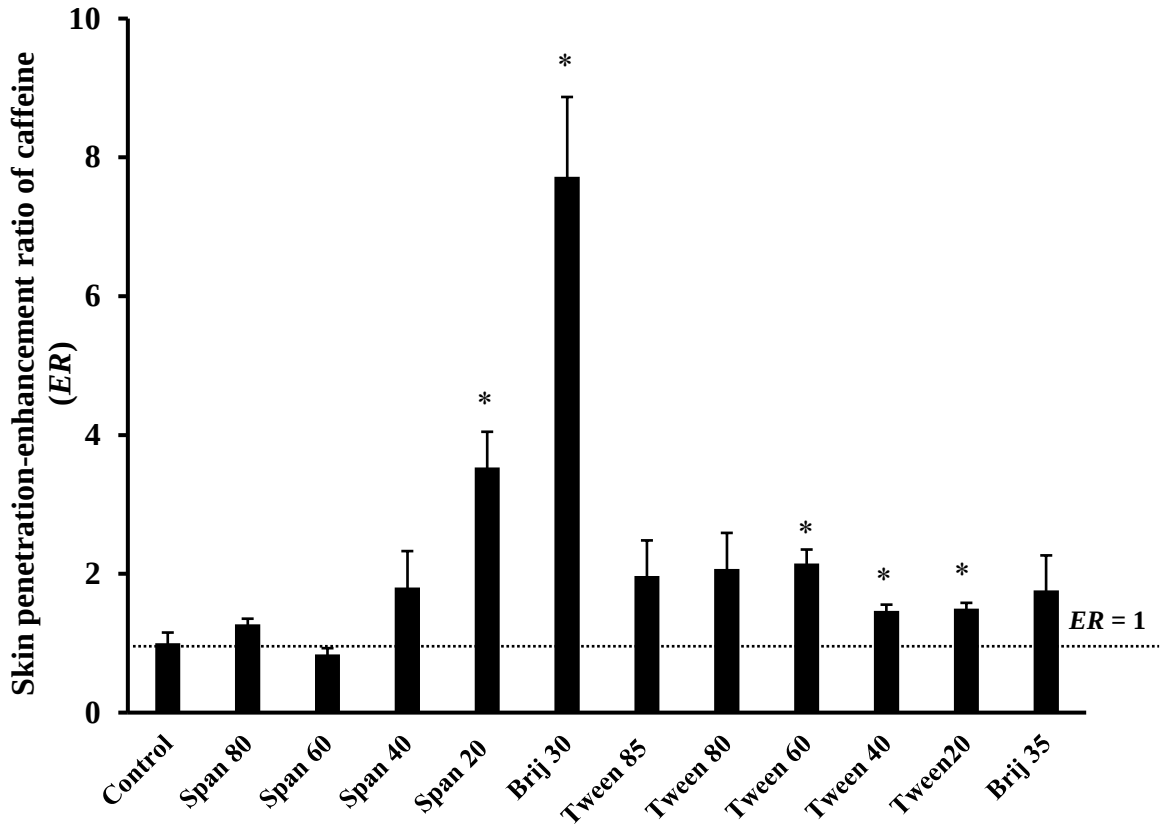

Fig. 2-3. *ER* of caffeine permeation through skin from different non-ionic surfactants dispersion. Each value represents the mean ± S.E. (n = 3–4). *: $p < 0.05$ significantly different from control.

2.3.2. Characteristics of liposomes and niosomes

Table 2-1 shows the characteristics of various types of liposomes and niosomes prepared in this study. All liposome formulations had a small diameter in a range of 110-185 nm. Phosphatidylcholine (DLPC, DMPC, DPPC, DSPC, DOPC) liposomes showed larger particle size than phosphatidylglycerol (DLPG, DMPG, DPPG, DSPG and DOPG) liposomes. The zeta potential of these phosphatidylcholine liposomes had quite neutral charge, whereas phosphatidylglycerol liposomes had negatively surface charge less than -40 mV. The *EE* was less than 50% and T_m was within a range of 41-66°C for all liposomes.

For niosomes, Span niosomes showed bigger particle size than Tween and Brij niosomes. This may be due to different hydrophilicity/hydrophobicity of the non-ionic surfactants. The zeta potential of niosomes was different depending on the type of non-ionic

surfactants used. The *EE* in all niosomes was low. Only Tween 60 niosomes could reach 33.9%. T_m of all niosomes was within a range of 11-28°C. Brij 30 dispersion could provide high *ER*, although niosomes were not formed (the oil droplet segregation was observed).

Table 2-1. Characteristics of liposomes and niosomes

Main component		T_m (°C)	*EE* (%)	Particle diameter (nm)	Polydispersity Index	Zeta potential (mV)
DLPC	(12:0)	49.8	15.44 ± 0.74	161.2 ± 0.3	0.211 ± 0.023	0.2 ± 0.5
DLPG	(12:0)	-	23.98 ± 0.42	109.3 ± 0.3	0.088 ± 0.016	-41.2 ± 3.0
DMPC	(14:0)	49.0	18.68 ± 0.54	165.3 ± 2.0	0.111 ± 0.079	-1.3 ± 1.6
DMPG	(14:0)	65.3	27.95 ± 1.10	130.2 ± 0.8	0.059 ± 0.011	-40.3 ± 3.5
DPPC	(16:0)	47.6	17.46 ± 0.63	169.9 ± 2.4	0.250 ± 0.011	-1.3 ± 0.7
DPPG	(16:0)	41.5	13.35 ± 0.03	152.1 ± 0.9	0.164 ± 0.016	-44.3 ± 2.5
DSPC	(18:0)	51.7	12.93 ± 0.15	184.6 ± 3.4	0.214 ± 0.005	-0.5 ± 1.2
DSPG	(18:0)	62.8	21.14 ± 0.27	162.1 ± 0.9	0.096 ± 0.007	-45.1 ± 1.0
DOPC	(18:1)	65.8	49.08 ± 1.27	143.3 ± 1.0	0.070 ± 0.007	-6.6 ± 1.2
DOPG	(18:1)	54.5	45.38 ± 0.11	110.7 ± 0.5	0.116 ± 0.122	-41.6 ± 1.7
Span 80		27.7	7.8	343.4 ± 31.7	0.313 ± 0.018	-22.3 ± 0.7
Span 40		24.5	2.0	410.7 ± 15.2	0.239 ± 0.015	-20.2 ± 1.2
Span 20		25.4	3.6	342.9 ± 18.9	0.236 ± 0.029	-12.6 ± 0.6
Tween 85		11.5	8.0	77.2 ± 0.2	0.103 ± 0.006	-10.5 ± 0.1
Tween 60		24.5	33.9	119.4 ± 1.3	0.125 ± 0.008	-3.8 ± 0.2
Brij 35		40.6	4.1	122.7 ± 0.2	0.132 ± 0.011	-1.6 ± 0.4

Each value represents the mean ± S.D.

2.3.3. Skin permeation of caffeine from liposomes and niosomes

Liposomes and niosomes prepared from different phospholipids/non-ionic surfactants were determined for their skin penetration-enhancing of caffeine. Time course of the cumulative amount of caffeine that permeated through skin from different kinds of liposomes and niosomes over 8 h are shown in Figs. 2-4 and 2-5. Typical lag time and following steady-state permeation profiles were observed for all liposome preparations prepared in this experiment. Only DPPG, DLPC and DMPC liposomes significantly promoted the caffeine permeation compared to control (*ER* was 5.43, 3.17 and 2.17, respectively), whereas DPPC and DOPG liposomes decreased the caffeine permeation (*ER* was 0.21 and 0.27, respectively). No or little change in the skin permeation was found by the other phospholipid liposomes. For

niosomes, on the other hand, two types of niosomes including Span 20 and Tween 85 niosomes could significantly increase the skin permeation of caffeine as compared to control solution (*ER* 2.99 and 2.69, respectively).

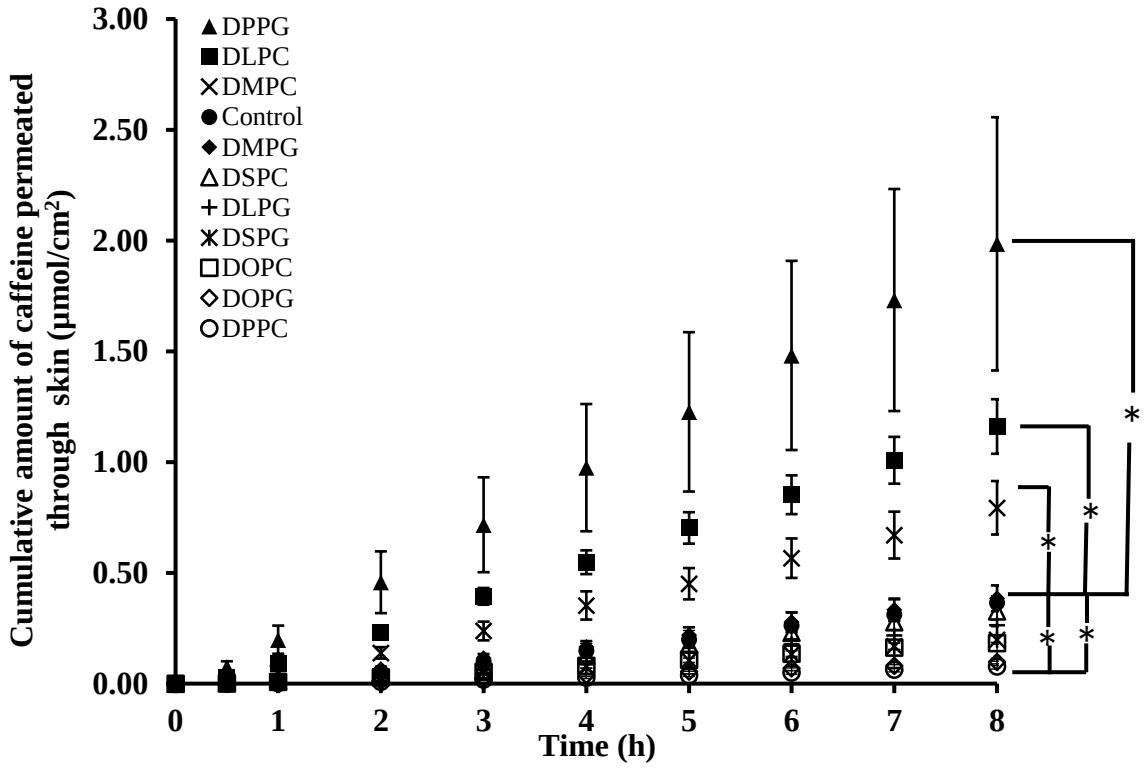

Fig. 2-4. Skin permeation profile of caffeine from different liposome formulations. Each value represents the mean ± S.E. (n = 3-5). *: $p < 0.05$ significantly different from control (free caffeine solution in PBS).

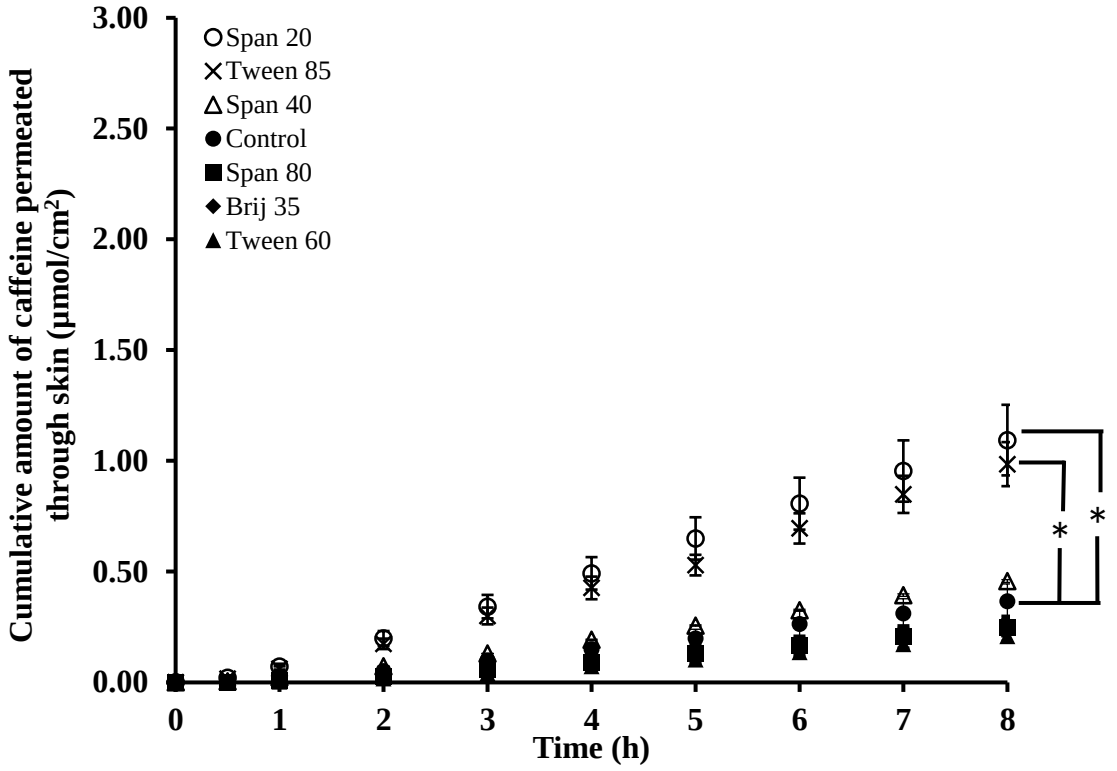

Fig. 2-5. Skin permeation profile of caffeine from different niosome formulations. Each value represents the mean ± S.E. (n = 3-5). *: $p < 0.05$ significantly different from control (free caffeine solution in PBS).

Then, the skin penetration-enhancing effect by phospholipids/non-ionic surfactant dispersions and their liposomes/niosomes were compared as shown in Figs. 2-6 and 2-7. DLPC, DMPC and DPPG liposomes showed significant higher *ER* compared to their phospholipid dispersions, while DPPC and DSPC liposomes showed significant lower *ER*.

Although DSPC phospholipid provided the highest *ER* in the form of dispersion, the skin permeation of caffeine from DSPC liposomes was substantially decreased. DPPG showed the enhancement effect both by phospholipid dispersion and liposome. However, its *ER* was highly increased by modification into the liposome formulation. In cases of other phospholipids such as DLPG, DMPG, DSPG, DOPC and DOPG, their liposomes showed no significant difference in the *ER* to those from their dispersions.

The *ER* from all niosomes did not enhance compared to their dispersions. Especially Span 80 and Tween 60 niosomes provided significant lower *ER* than their dispersions.

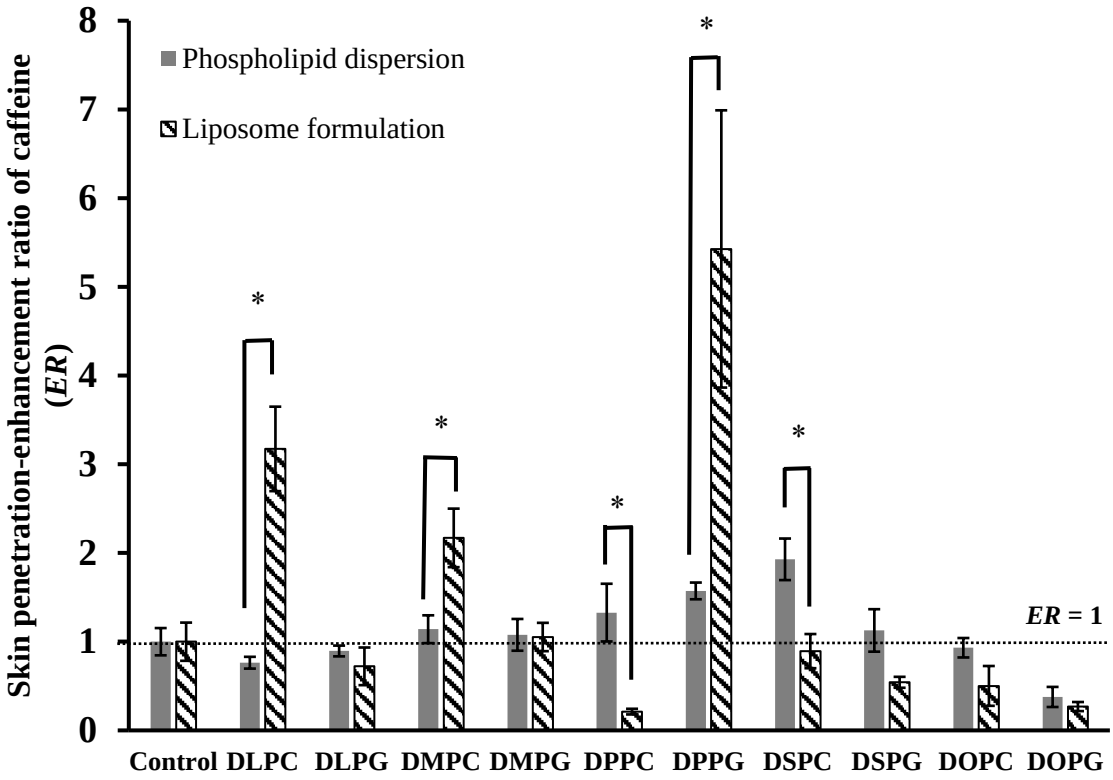

Fig. 2-6. Comparison of *ER* of caffeine permeation obtained from phospholipid dispersions and liposomes. Each value represents the mean ± S.E. (n = 3–5). *: $p < 0.05$ significantly different from its phospholipid dispersion.

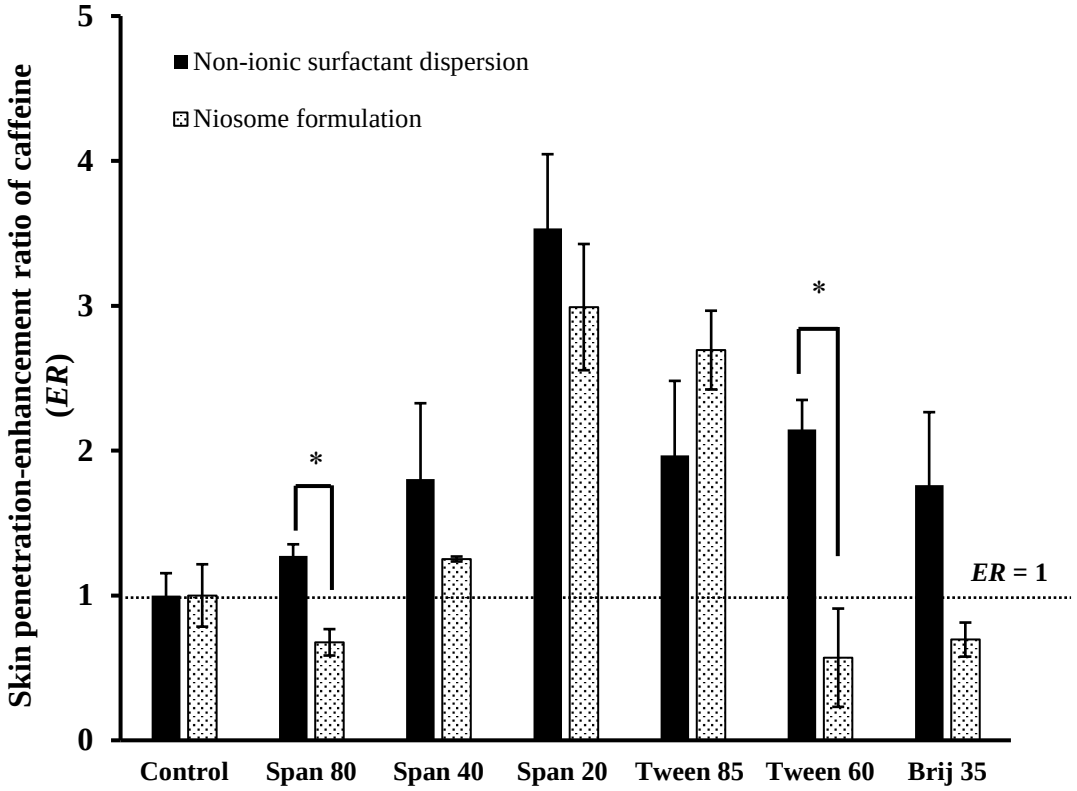

Fig. 2-7. Comparison of *ER* of caffeine permeation obtained from non-ionic surfactants dispersions and niosomes. Each value represents the mean ± S.E. (n = 3–5). *: $p < 0.05$ significantly different from its non-ionic surfactant dispersion.

2.3.4. Effect of pretreatment with caffeine-free phospholipid dispersions and liposomes on the skin permeation of caffeine

DPPG and DLPC liposomes exhibited the highest skin penetration-enhancing effects among all liposomes, but DSPG liposomes exhibited low skin permeation of caffeine. Then these three phospholipids were selected and 1 h-pretreatment experiment was done before skin permeation experiment from caffeine solution to clarify the possible effect of liposomes on the skin permeation of caffeine. As results, the pretreatment with phospholipid dispersions enhanced caffeine permeation for DLPC (*ER* = 1.35) and DPPG (*ER* = 2.47), but decreased for DSPG (*ER*=0.48) as shown in Fig. 2-8.

The pretreatment experiment was also performed using caffeine-free liposomes. Interestingly, the 1 h-pretreatment with caffeine-free liposomes showed different results: the lower *ER* was observed compared to the effect of pretreatment with phospholipids dispersions. The *ER* for caffeine-free DLPC, DPPG and DSPG liposomes were 0.87, 1.50 and 0.46, respectively, as shown in Fig. 2-8.

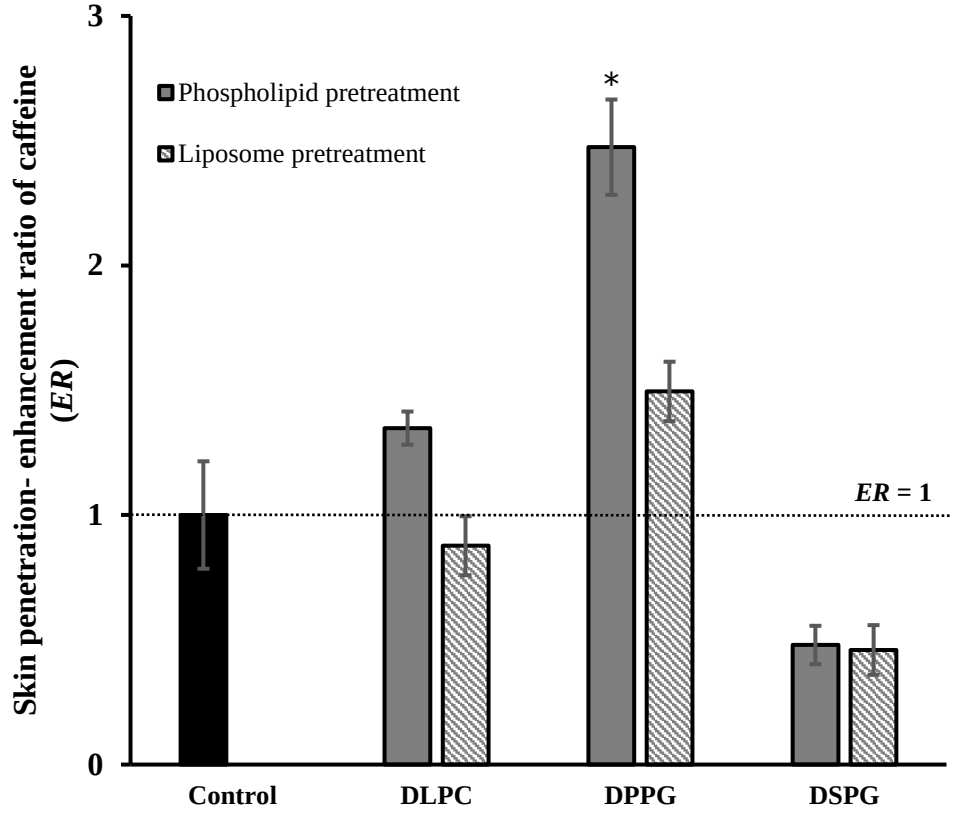

Fig. 2-8. Effect of 1 h-pretreatment with caffeine-free phospholipid dispersions and liposomes on the *ER* of skin permeation of caffeine. Each value represents the mean ± S.E. (n = 3–5).
*: $p < 0.05$ significantly different from control (no pretreatment; free caffeine solution in PBS).

2.3.5. Effect of physical mixture of blank liposomes and caffeine solution (caffeine-spiked liposomes) on the skin permeation of caffeine

In order to evaluate the contribution of caffeine contents in the inside and outside of liposomes on its skin permeation, physical mixture of blank liposomes and caffeine was applied on the excised skin to measure the skin permeation of caffeine. The results are shown in Fig. 2-9. Caffeine-spiked DLPC or DSPG liposomes exhibited lower skin permeation of caffeine (*ER* was 0.58 and 0.44, respectively). On the other hand, only caffeine-spiked DPPG liposomes

significantly enhanced the skin permeation of caffeine (*ER* = 2.65) compared to control caffeine solution.

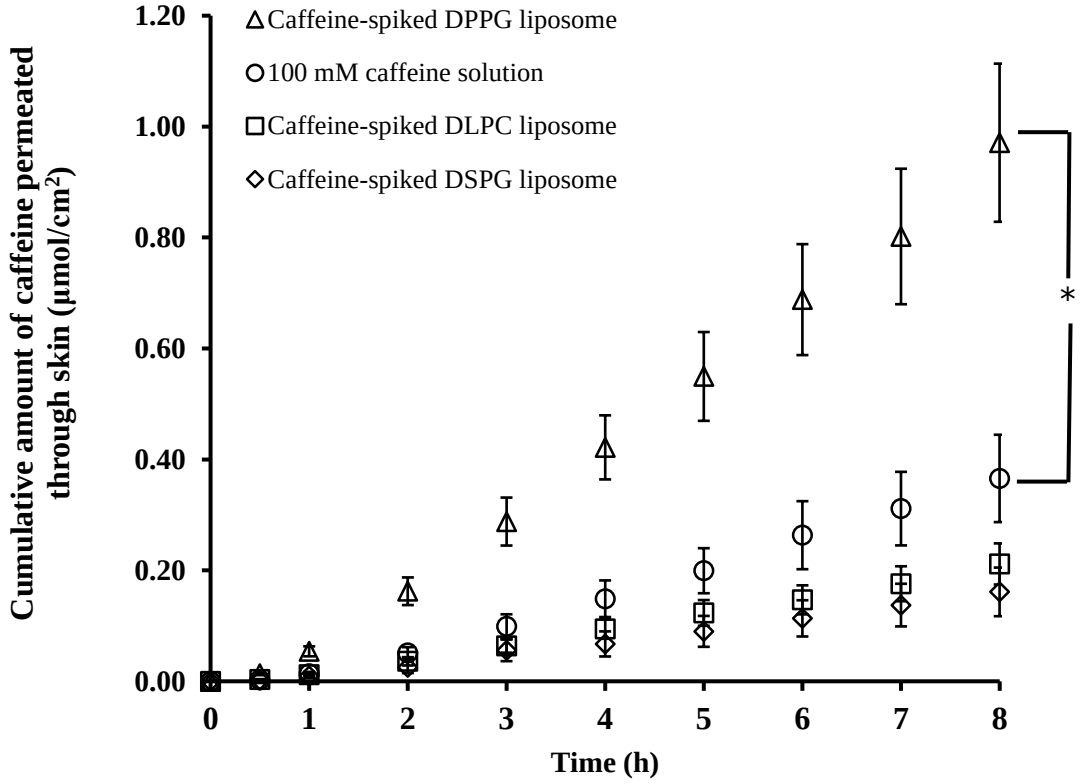

Fig. 2-9. Time course of the cumulative amount of caffeine that permeated through skin from physical mixture of blank liposomes and caffeine solution (caffeine-spiked DPPG, DLPC and DSPG liposomes). Each value represents the mean ± S.E. (n = 3–5). *: $p < 0.05$ significantly different from control (free caffeine solution in PBS).

2.3.6. Effect of caffeine-entrapped liposomes on the skin permeation of caffeine

Next, caffeine-entrapped liposomes were evaluated and the skin permeation data for caffeine was shown in Fig. 2-10. Caffeine-entrapped DPPG liposomes showed the highest caffeine permeation (*ER* = 4.39), whereas caffeine-entrapped DLPC liposomes enhanced about 1.65-fold compared to caffeine solution which contained the same concentration as in liposome formulations. No penetration enhancing effect was observed for the caffeine-entrapped DSPG liposomes.

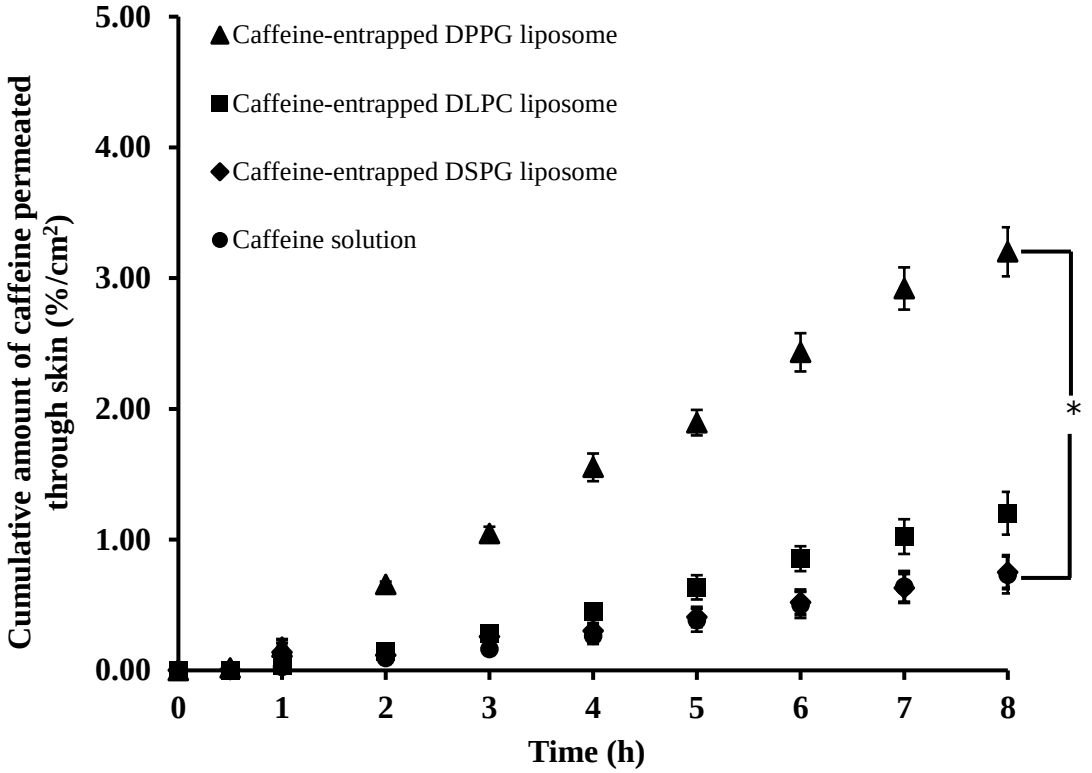

Fig. 2-10. Time course of the normalized cumulative amount of caffeine that permeated through skin from caffeine-entrapped DPPG, DLPC and DSPG liposomes. Each value represents the mean ± S.E. (n = 3–5). *: $p < 0.05$ significantly different from control (free caffeine solution in PBS). Y-axis was calculated with dividing the cumulative amount of caffeine that permeated through skin by the total amount of applied drug.

2.4. Discussion

Although several studies have reported on the potential of vesicular carriers including liposomes and niosomes as a topical/transdermal drug delivery system compared to conventional formulations[56,69,70], there seems to be a general lack of understanding among researchers regarding on the formulation factors of liposomes and niosomes to provide high skin penetration-enhancing effect. Therefore, the present study was mainly focused on the designing strategies of liposome and niosome formulations by investigating the effect of their compositions on the enhanced skin permeation of drugs.

In the present study, skin penetration-enhancing effect of different phospholipids and non-ionic surfactants was evaluated using caffeine as a model penetrant, since the selection of

phospholipids and non-ionic surfactants must be very important to design suitable vesicle formulations. The skin permeation of caffeine was significantly improved by DPPG and DSPC dispersions, whereas DOPG dispersion markedly decreased the skin permeation. In addition, the other phospholipids had no or little skin penetration-enhancing effects against the control group (Fig. 2-2). On the other hand, significant improvement in skin permeation of caffeine was observed with Span 20, Brij 30, Tween 20, 40 and 60 compared to other non-ionic surfactants. These results strongly supported the concept of the present study, Thus, the vesicle compositions in the liposome or niosome formulations must be considered in the development of such formulations (Fig. 2-3).

In addition, the prepared liposomes and niosomes had a small size (80-410 nm). T_m, *EE* and zeta potential were dramatically affected by changes of phospholipid/ non-ionic surfactant compositions (Table 2-1). However, the reason for the differences in the skin penetration-enhancing effects depending on the compositions is still unknown.

Next, the skin penetration-enhancement effect of liposome and niosome formulations was evaluated (Fig. 2-4). The reason why only three liposome formulations made of DPPG, DLPC and DMPC showed higher skin permeation than other liposome formulations and control solution can be explained as follow, 1) Some liposomes might have a rigid structure that could form an extra lipid barrier onto the skin surface which retards the skin permeation of caffeine, and this extent must be different depending on the phospholipids, or 2) some liposomes might release caffeine in a slower rate than other phospholipid-based liposomes probably due to the interaction between the drug and phospholipids[71].

On the other hand, the same kind of findings were observed in the case of niosome formulations (Fig. 2-5). Only Span 20 and Tween 85 niosomes showed significant skin penetration-enhancing effect for caffeine, indicating that the selected type of non-ionic surfactants in niosome formulations could influence the skin permeation of drugs.

As a comparison, the skin penetration-enhancement ratios (*ER*) that obtained from the phospholipid dispersions were different from their liposome formulations (Fig. 2-6), suggesting that liposome vesicles containing caffeine have different mechanisms to increase the skin permeation than the phospholipid dispersions. Interestingly, DPPG dispersion as well as its liposome formulation resulted in high *ER* of caffeine, indicating that the DPPG is a promising phospholipid to fabricate liposomes. The same phenomenon was observed in the

case of niosome formulations. The performance of these formulations was affected by their compositions (Fig. 2-7). The non-ionic surfactant dispersions of Span 20 and Tween 85 as well as their niosomes showed high *ER* of caffeine, indicating that these non-ionic surfactants are very promising ones to develop niosomes. Further studies are necessary to fully understand the reason for the differences in the skin penetration-enhancement effects beween phospholipid/non-ionic surfactants and their liposomes/niosomes as well as among different compositions.

To further understand the possible mechanism of action of each phospholipid, the skin pretreatment approach and following skin permeation experiment of caffeine were carried out using caffeine-free phospholipid dispersions and liposomes (Fig. 2-8). In addition, the effect of physical mixture of blank liposomes and caffeine solution (caffeine-spiked liposomes) (Fig. 2-9) and caffeine-entrapped liposomes (caffeine presented only in the liposomes) (Fig. 2-10) were determined. Pretreatment with DLPC and DPPG dispersions enhanced the skin permeation of caffeine, indicating that these phospholipids had skin penetration-enhancing effects, since they might mix and fuse with the SC lipids (like ceramides) to reduce the SC barrier function made by well-packed intercellular lipids and create a permeation pathway for drugs[61,72,73]. Interestingly, the pretreatment of caffeine-free liposomes provided lower *ER* than their corresponding phospholipid dispersions. This could be due to the presence of such vesicles having less fluidity to disrupt the rigid structure of SC than its dispersion forms. Obviously, only the pretreatment with caffeine-free DPPG liposomes increased the skin permeation of caffeine. For the physical mixture of blank liposomes and caffeine, caffeine-spiked DPPG liposomes could deliver the drug through skin with the highest *ER*. Caffeine-free DPPG liposomes might disrupt the SC structure, allowing the free caffeine being mixed outside the liposome vesicles to diffuse through the skin barrier. In consequence, the caffeine-entrapped DPPG liposomes also provided the highest *ER* compared to the caffeine-entrapped DLPC and DSPG liposomes (Fig. 2-10).

The highest skin penetration-enhancing effect observed from DPPG liposomes was thus due to the synergistic of different actions; the skin penetration-enhancing effect of DPPG dispersions and the skin-penetration enhancing effect of caffeine-free DPPG liposomes as well as the penetration-enhancing ability of caffeine both outside (caffeine-spiked liposome) and inside (caffeine-entrapped liposome) of liposomal vesicles. As similar to the previous report[74], the penetration of non-entrapped and entrapped hydrophilic fluorescence probe, carboxyfluorescein, in liposomes through human skin were increased compared to control

solution. The fluorescent may be penetrated along with intact liposomes or associated with liposomal fragment. The skin penetration-enhancing effect of DLPC liposomes was obtained in spite of only a low degree, and no skin penetration-enhancing effect was observed for DSPG liposomes in all cases. However, DPPG was a very promising candidate to design liposome formulations to enhance the drug permeation compared to other phospholipids.

2.5. Chapter conclusion

Our findings exhibited that the vesicle composition of liposomes and niosomes is an important factor that should be considered by researchers in this field in order to improve the performance of these formulations. Understanding the effect of such factor on the performance of liposome and niosome formulations could enable researchers to develop the effective formulations to improve the skin permeation of drugs.

Conclusion

The following conclusion can be obtained from the present results:

(1) SCLLs could be used as a model membrane instead of hairless rat skin to investigate the skin penetration-enhancing effect of CPEs. Fair correlation was observed between increase in *ER* and FL leakage/ SCLLs membrane fluidity when using ethanol as a model CPE.
(2) Use of SCLLs could be a promising approach to determine the effect of various kinds of CPEs on the SC skin barrier. The relationship between FL leakage and SCLLs membrane fluidity could be utilized to identify the possible mechanism of action of CPEs for enhancing the skin permeation of drugs. This approach is useful for testing of CPEs in an early stage of development of transdermal/topical formulations.
(3) Selection of vesicle compositions is an important strategy for preparation of vesicular carriers aimed to enhance skin permeation of hydrophilic model drug. Understanding the effect of such factors could enable researchers to develop vesicular carriers that intended to improve the skin permeation of drugs.

These results obtained in the present study strongly suggested that SCLLs could be used as a model skin membrane. In addition, the composition of vesicles must be considered as an optimized parameter for enhancing the skin penetration of drugs.

Acknowledgement

I would like to express my deepest appreciation to my research supervisor, Prof. Kenji Sugibayashi, for his wise advices, encouragement, motivation, and for sharing his immense knowledge. He was my inspiration that I desired.

I am grateful to Assoc. Prof. Hiroaki Todo and Assistant Mr. Wesam Radhi Kadhum for their valuable insights throughout the research as well as their guidance in the presentation and writing processes.

I would like to express my sincere gratitude to vice research supervisors, Prof. Hideo Ueda and Prof. Yoichiro Arata for their helpful advices.

I also would like to thank you Ms. Megumi Fukasawa, Ms. Akie Okada and Mr. Yuki Kitao for their assistance in the best techniques in liposome research and for being good colleages.

Members of the Laboratory of Pharmaceutics and Cosmeceutics who formed part of my academic success. Thank you for the experimental techniques they taught, along with all the extra-curricular activities we did together were truly precious moments.

I also very much appreciate to Walailak University, for the financial support to me to pursue the great opportunity of studying Ph.D. in Japan.

The essential experimental animals sacrificed during my study are also greatly remembered.

Finally, this accomplishment cannot be possible without the love, understanding and support of my family. Their love strengthened me whenever I fall.

References

1. Naik A., Kalia Y. N., Guy R. H., Transdermal drug delivery: overcoming the skin's barrier function, *Pharm. Sci. Technolo. Today*, **3**, 318-326 (2000).
2. Shilakari G., Singh D., Asthana A., Novel vesicular carriers for topical drug delivery and their application's, *Int. J. Pharm. Sci. Rev. Res.*, **21**, 77-86 (2013).
3. Denet A., Vanbever R., Preat V., Skin electroporation for transdermal and topical delivery, *Adv. Drug Deliv. Rev.*, **56**, 659–674 (2004).
4. Alexander A., Ajazuddin D. S., Giri T. K., Saraf S., Saraf S., Tripathi D. K., Approaches for breaking the barriers of drug permeation through transdermal drug delivery, *J. Control. Release*, **164**, 26–40 (2012).
5. Liu K. S., Sung K. C., Al-Suwayeh S. A., Ku M. C., Chu C. C., Wang J. J., Fang J. Y., Enhancement of transdermal apomorphine delivery with a diester prodrug strategy, *Eur. J. Pharm. Biopharm.*, **78**, 422–431 (2011).
6. Taghizadeh S. M., Moghimi-Ardakani A., Mohamadnia F., A statistical experimental design approach to evaluate the influence of various penetration enhancers on transdermal drug delivery of buprenorphine, *J. Adv. Res.*, **6**, 155–162 (2015).
7. Jadhav S. M., Morey P., Karpe M., Kadam V., Novel vesicular system: an overview, *J. Appl. Pharm. Sci.*, **2**, 193-202 (2012).
8. Karande P., Jain A., Mitragotri S., Relationships between skin's electrical impedance and permeability in the presence of chemical enhancers, *J. Control. Release*, **110**, 307-313 (2006).
9. Sugibayashi K., Hosoya K., Morimoto Y., Higuchi W. I., Effect of the absorption enhancer, Azone, on the transport of 5-fluorouracil across hairless rat skin, *J. Pharm. Pharmacol.*, **37**, 578-580 (1985).
10. El Maghraby G. M., Barry B. W., Williams A. C., Liposomes and skin: From drug delivery to model membranes, *Eur. J. Pharm. Sci.*, 34, 203-222 (2008).
11. Suhonen M., Li S. K., Higuchi W. I., Herron J. N., A liposome permeability model for stratum corneum lipid bilayers based on commercial lipids, *J. Pharm. Sci.*, **97**, 4278-4293 (2008).
12. Rajan R., Jose S., Mukund V. P. B., Vasudevan D. T., Transferosomes - A vesicular transdermal delivery system for enhanced drug permeation, *J. Adv. Pharm. Tech. Res.,* **2**, 138-143 (2011).

13. Honeywell-Nguyen P. L., Bouwstra J. A., Vesicles as a tool for transdermal and dermal delivery, *Drug Discov. Today*, **2**, 67-74 (2005).
14. Elsayed M. M. A., Abdallah O. Y., Naggar V. F., Khalafallah N. M., Lipid vesicles for skin delivery of drugs: Reviewing three decades of research. *Int. J. Pharm*., **332**, 1–16 (2007).
15. Kirjavainen M., Monkkonen J., Saukkosaari M., Valjakka-Koskela R., Kiesvaara J., Urtti A., Phospholipids affect stratum corneum lipid bilayer fluidity and drug partitioning into the bilayers, *J. Control. Release*, **58**, 207–214 (1999).
16. Smeden J. V., Janssens M., Gooris G. S., Bouwstra J. A., The important role of stratum corneum lipids for the cutaneous barrier function, *Biochim. Biophys. Acta*, **1841**, 295-313 (2014).
17. Wertz P. W., Bergh B. V. D., The physical, chemical and functional properties of lipids in the skin and other biological barriers, *Chem. Phys. Lipids,* **91**, 85-96 (1998).
18. Wertz P. W., Lipids and function barrier of the skin, *Acta Derm-Venereol. Suppl.*, **208**, 7-11 (2000).
19. Barry B. W., Mode of action of penetration enhancers in human skin, *J. Control. Release,* **6**, 85-97 (1987).
20. Wertz P. W., Abraham W., Landmann L., Downing D. T., Preparation of liposomes from stratum corneum lipids, *J. Invest. Dermatol.*, **87**, 582-584 (1986).
21. Kim C. K., Hong M. S., Kim Y. B., Han S. K., Effect of penetration enhancers (pyrrolidone derivatives) on multilamellar liposomes of stratum corneum lipid: a study by UV spectroscopy and differential scanning calorimetry, *Int. J. Pharm*., **95**, 43-50 (1993).
22. El Maghraby G. M. M., Campbell M., Finnin B., Mechanisms of action of novel skin penetration enhancers: phospholipid versus skin lipid liposomes, *Int. J. Pharm*., **305**, 90-104 (2005).
23. Yoneto K., Li S. K., Ghanem A. H., Crommelin D. J., Higuchi W. I., A mechanistic study of the effects of the 1-alkyl-2-pyrrolidones on bilayer permeability of stratum corneum lipid liposomes: a comparison with hairless mouse skin studies, *J. Pharm. Sci*., **84**, 853-861 (1995).
24. Suhonen T. M., Pirskanen L., Raisanen M., Kosonen K., Rytting J. H., Paronen P., Urtti A., Transepidermal delivery of β-blocking agents: evaluation of enhancer effects using stratum corneum lipid liposomes, *J. Control. Release,* **43**, 251-259 (1997).

25. Yoneto K., Li S. K., Higuchi W. I., Jiskoot W., Herron J. N., Fluorescent probe studies of the interactions of 1-alkyl-2-pyrrolidones with stratum corneum lipid liposomes, *J. Pharm. Sci*., **85**, 511-517 (1996).
26. Berner B., Mazzenga G. C., Otte J. H., Steffens R. J., Juang R. H., Ebert C. D., Ethanol: water mutually enhanced transdermal therapeutic system II. Skin permeation of ethanol and nitroglycerin, *J. Pharm. Sci*., **78**, 402-407 (1989).
27. Friend D., Catz P., Heller J., Reid J., Baker R., Transdermal delivery of levonorgestrel I. Alkanols as permeation enhancer, *J. Control. Release*, **7**, 243-250 (1988).
28. Pershing L. K., Lambert L. D., Knutson K., Mechanism of ethanol-enhanced estradiol permeation across human skin in vivo, *Pharm. Res.*, **7**, 170-175 (1990).
29. Hatfield R. M., Fung L. W. M., Molecular properties of a stratum corneum model lipid system: large unilamellar vesicles, *Biophys. J.*, **68**, 196–207 (1995).
30. Tan C., Feng B., Zhang X., Xia W., Xia S., Biopolymer-coated liposomes by electrostatic adsorption of chitosan (chitosomes) as novel delivery systems for carotenoids, *Food Hydrocolloid.*, **52**, 774-784 (2016).
31. Tan C., Xia S., Xue J., Xie J., Feng B., Zhang X., Liposomes as vehicles for lutein: preparation, stability, liposomal membrane dynamics, and structure, *J. Agric. Food Chem.*, **34**, 8175-8184 (2013).
32. Imura T., Sakai H., Yamauchi H., Kaise C., Kozawa K., Yokoyama S., Abe M., Preparation of liposomes containing Ceramide 3 and their membrane characteristics, *Colloid. Surface. B.*, **20**, 1–8 (2001).
33. Freitas C., Müller R. H., Effect of light and temperature on zeta potential and physical stability in solid lipid nanoparticle dispersions, *Int. J. Pharm.*, **168**, 221-229 (1998).
34. Barry B. W., Lipid-Protein-Partitioning theory of skin penetration enhancement, *J. Control. Release*, **15**, 237-248 (1991).
35. Sugibayashi K., Nemoto M., Morimoto Y., Effect of several penetration enhancers on the percutaneous absorption of indomethacin in hairless rats, *Chem. Pharm. Bull*., **36**, 1519-1528 (1988).
36. Williams A. C., Barry B. W., Penetration enhancers, *Adv. Drug Deliv. Rev*., **64**, 128-137 (2012).
37. Horita D., Todo H., Sugibayashi K., Effect of ethanol pretreatment on skin penetration of drugs, *Biol. Pharm. Bull*., **35**, 1343-1348 (2012).

38. Horita D., Hatta I., Yoshimoto M., Kitao Y., Todo H., Sugibayashi K., Molecular mechanisms of action of different concentrations of ethanol in water on ordered structures of intercellular lipids and soft keratin in the stratum corneum, *Biochim. Biophys. Acta*, **1848**, 1196-1202 (2015).
39. Lane M. E., Skin penetration enhancers, *Int. J. Pharm.*, **447**, 12-21 (2013).
40. Michelon M., Mantovani R. A., Sinigaglia-Coimbra R., de la Torre L. G., Cunha R. L., Structural characterization of β-carotene-incorporated nanovesicles produced with non-purified phospholipids, *Food Res. Int.*, **79**, 95-105 (2016).
41. Dayan N., Touitou E., Carriers for skin delivery of trihexyphenidyl HCl: ethosomes vs. liposomes, *Biomaterials*, **21**, 1879-1885 (2000).
42. Peng A., Pisal D. S., Doty A., Balu-lyer S. V., Phosphatidylinositol induces fluid phase formation and packing defects in phosphatidylcholine model membranes, *Chem. Phys. Lipids*, **165**, 15-22 (2012).
43. Ongpipattanakul B., Burnette R. R., Potts R. O., Francoeur M. L., Evidence that oleic acid exists in a separate phase within stratum corneum lipids, *Pharm. Res*., **7**, 350-354 (1991).
44. Rowat A. C., Kitson N., Thewalt J. L., Interactions of oleic acid and model stratum corneum membranes as seen by ^{2}H NMR, *Int. J. Pharm*., **307**, 225–231 (2006).
45. Walters K. A., Walker M., Olejnik O., Non-ionic surfactant effects on hairless mouse skin permeability characteristics, J. Pharm. Pharmacol., **40**, 525–529 (1987).
46. Lane M. E., Santos P., Watkinson A. C., Hadgraft J., "Transdermal and topical drug delivery", Chap. 2, ed. by Benson H. A. E., Watkinson A. C., A John Wiley & Sons, Inc., New Jersey, 23-42 (2012).
47. Kwak S., Brief E., Langlais D., Kitson N., Lafleur M., Thewalt J., Ethanol perturbs lipid organization in models of stratum corneum membranes: An investigation combining differential scanning calorimetry, infrared and ^{2}H NMR spectroscopy, *Biochim. Biophys. Acta*, **1818**, 1410-1419 (2012).
48. Barry B. W., Novel mechanisms and devices to enable successful transdermal drug delivery, *Eur. J. Pharm. Sci*., **2**, 101-111 (2001).
49. Hatta I., Nakazawa H., Obata Y., Ohta N., Inoue K., Yagi N., Novel method to observe subtle structural modulation of stratum corneum on applying chemical agents, *Chem. Phys. Lipids*, **163**, 381-389 (2010).
50. Anigbogu A. N. C., Williams A. C., Barry B. W., Edwards H. G. M., Fourier transform raman spectroscopy of interactions between the penetration enhancer dimethyl sulfoxide and human stratum corneum, *Int. J. Pharm*., **125**, 265–282 (1995).

51. Greve T. M., Andersen K. B., Nielsen O. F., Penetration mechanism of dimethyl sulfoxide in human and pig ear skin: An ATR–FTIR and near-FT Raman spectroscopic in vivo and in vitro study, *Spectroscopy*, **22**, 405–417 (2008).
52. Brinkmann I., Muller-Goymann C. C., An attempt to clarify the influence of glycerol, propylene glycol, isopropyl myristate and a combination of propylene glycol and isopropyl myristate on human stratum corneum, *Pharmazie*, **60**, 215-220 (2005).
53. Williams A. C., Barry B. W., Penetration enhancers, *Adv. Drug Deliv. Rev.*, **56**, 603-618 (2004).
54. Som I., Bhatia K., Yasir M., Status of surfactants as penetration enhancers in transdermal drug delivery, *J. Pharm. Bioallied Sci.*, **4**, 2-9 (2012).
55. Yu H. Y., Liao H. M., Triamcinolone permeation from different liposome formulations through rat skin in vitro, *Int. J. Pharm*., **127**, 1-7 (1996).
56. Liu H., Pan W. S., Tang R., Luo S. D., Topical delivery of different acyclovir palmitate liposome formulations through rat skin in vitro, *Pharmazie*, **59**, 203-206 (2004).
57. Jain S., Patel N., Shah M. K., Khatri P., Vora N., Recent advances in lipid-based vesicles and particulate carriers for topical and transdermal application, *J. Pharm. Sci.*, **106**, 423-445 (2017).
58. El Maghraby G. M. M., Williams A. C., Barry B. W., Can drug-bearing liposomes penetrate intact skin, *J. Pharm. Pharmacol.* **58**, 415–429 (2006).
59. Marianecci C., Marzio L. D., Rinaldi F., Celia C., Paolino D., Alhaique F., Esposito S., Carafa M., Niosomes from 80s to present: The state of the art, *Adv. Colloid Interface Sci.*, **205**, 187–206 (2014).
60. Kato A., Ishibashi Y., Miyake Y., Effect of egg yolk lecithin on transdermal delivery of bunazosin hydrochloride, *J. Pharm. Pharmacol*., **39**, 399-400 (1987).
61. Kirjavainen M., Urtti A., Jaaskelainen I., Suhonen T.M., Paronen P., Valjakka-Koskela R., Kiesvaara J., Monkkonen J., Interaction of liposomes with human skin in vitro - the influence of lipid composition and structure, *Biochim. Biophys. Acta*, **1304**, 179-189 (1996).
62. Gillet A., Lecomte F., Hubert P., Ducat E., Evrard B., Piel G., Skin penetration behaviour of liposomes as a function of their composition, *Eur. J. Pharm. Biopharm*., **79**, 43–53 (2011).
63. Gillet A., Compere P., Lecomte F., Hubert P., Ducat E., Evrard B., Piel G., Liposome surface charge influence on skin penetration behavior, *Int. J. Pharm*., **411**, 223–231 (2011).

64. Verma D. D., Verma S., Blume G., Fahr A., Particle size of liposomes influences dermal delivery of substances into skin, *Int. J. Pharm.*, **258**, 141–151 (2003).
65. Touitou E., Dayan N., Bergelson L., Godin B., Eliaz M., Ethosomes — novel vesicular carriers for enhanced delivery: characterization and skin penetration properties, *J. Control. Release*, **65**, 403–418 (2000).
66. Duangjit S., Opanasopit P., Rojanarata T., Ngawhirunpa T., Characterization and in vitro skin permeation of meloxicam-loaded liposomes versus transfersomes, *J. Drug Deliv*., 9 pages (2011).
67. Manconi M., Caddeo C., Sinico C., Valenti D., Mostallino M. C., Biggio G., Fadda A. M., Ex vivo skin delivery of diclofenac by transcutol containing liposomes and suggested mechanism of vesicle–skin interaction, *Eur. J. Pharm. Biopharm.*, **78**, 27–35 (2011).
68. Michel C., Purmann T., Mentrup E., Seiller E., Kreuter J., Effect of liposomes on percutaneous penetration of lipophilic materials, *Int. J. Pharm*., **84**, 93-105 (1992).
69. Foldvari M., In vitro cutaneous and percutaneous delivery and in vivo efficacy of tetracaine from liposomal and conventional vehicles, *Pharm. Res*., **11**, 1593-1598 (1994).
70. Kirjavainen M., Urtti A., Valjakka-Koskela R., Kiesvaara J., Monkkonen J., Liposome–skin interactions and their effects on the skin permeation of drugs, *Eur. J. Pharm. Sci*., **7**, 279–286 (1999).
71. Zellmer S., Pfeil W., Lasch J., Interaction of phosphatidylcholine liposomes with the human stratum corneum, *Biochim. Biophys. Acta*, **1237**, 176-182 (1995).
72. Mahrhauser D. S., Reznicek G., Gehrig S., Geyer A., Ogris M., Kieweler R., Valenta C., Simultaneous determination of active component and vehicle penetration from F-DPPC liposomes into porcine skin layers, *Eur. J. Pharm. Biopharm.*, **97** 90-95 (2015).
73. Verma D. D., Verma S., Blume G., Fahr A., Liposomes increase skin penetration of entrapped and non-entrapped hydrophilic substances into human skin: a skin penetration and confocal laser scanning microscopy study, *Eur. J. Pharm. Biopharm*., **55**, 271–277 (2003).